Pulsations in close binaries: challenges and opportunities

Carla Maceroni INAF - OAR

INAF
ISTITUTO NAZIONALE DI ASTROFISICA
NATIONAL INSTITUTE FOR ASTROPHYSICS

The Space Photometry Revolution, Toulouse, July 10, 2014

The photometry revolution

B.C.
Ibanoglu et al. 2009, MNRAS

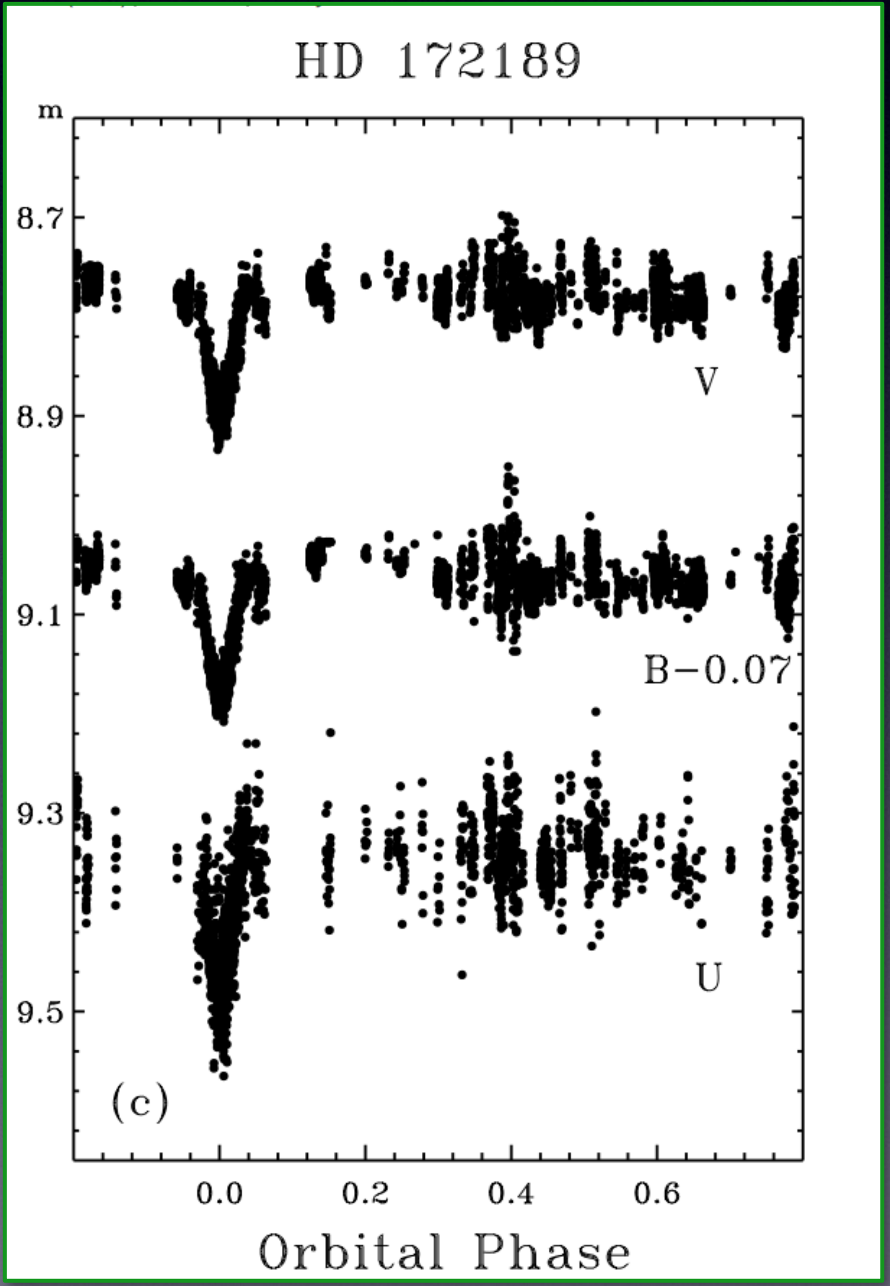

The photometry revolution

B.C.
Ibanoglu et al. 2009, MNRAS

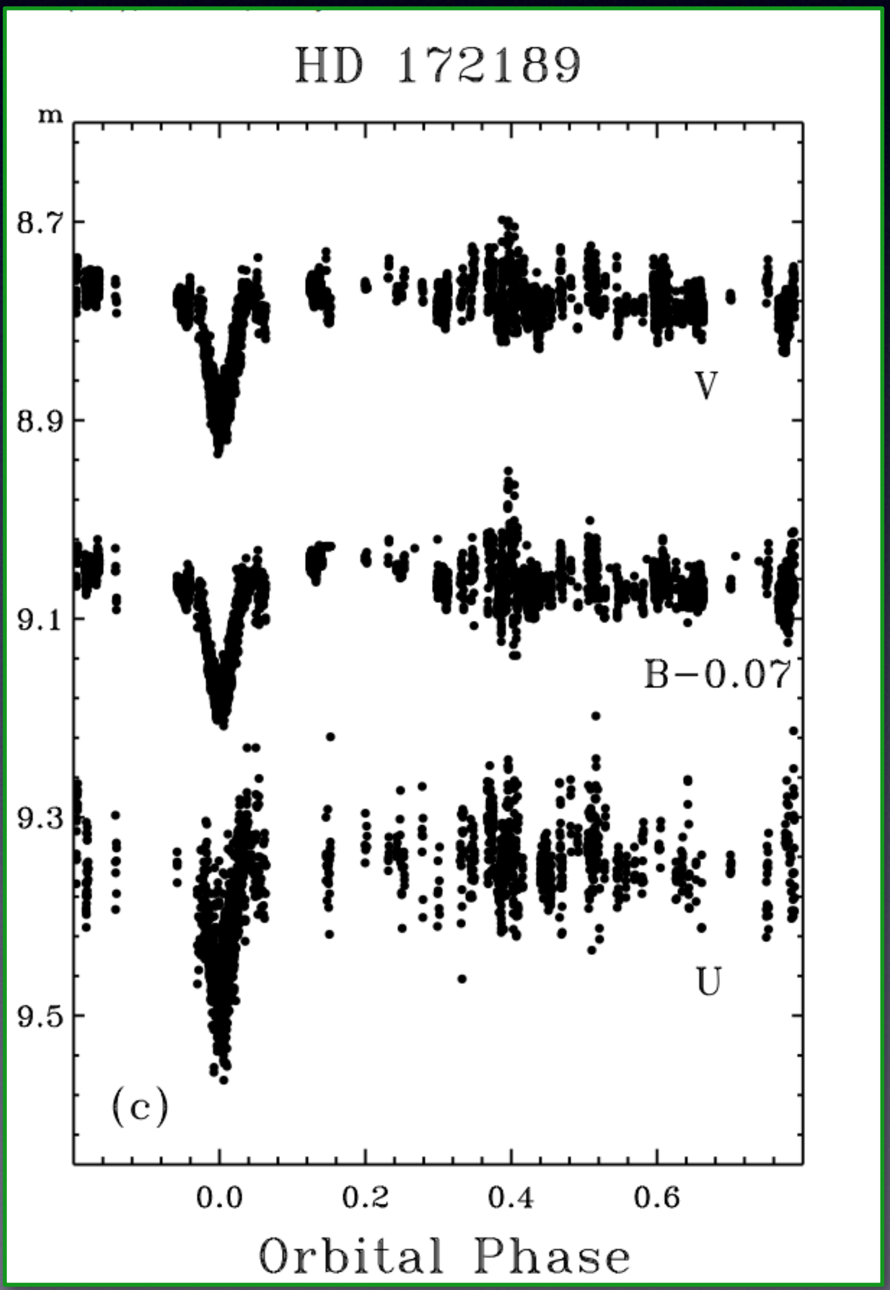

A.C.
CoRoT 8170 (a.k.a. HD 172189)

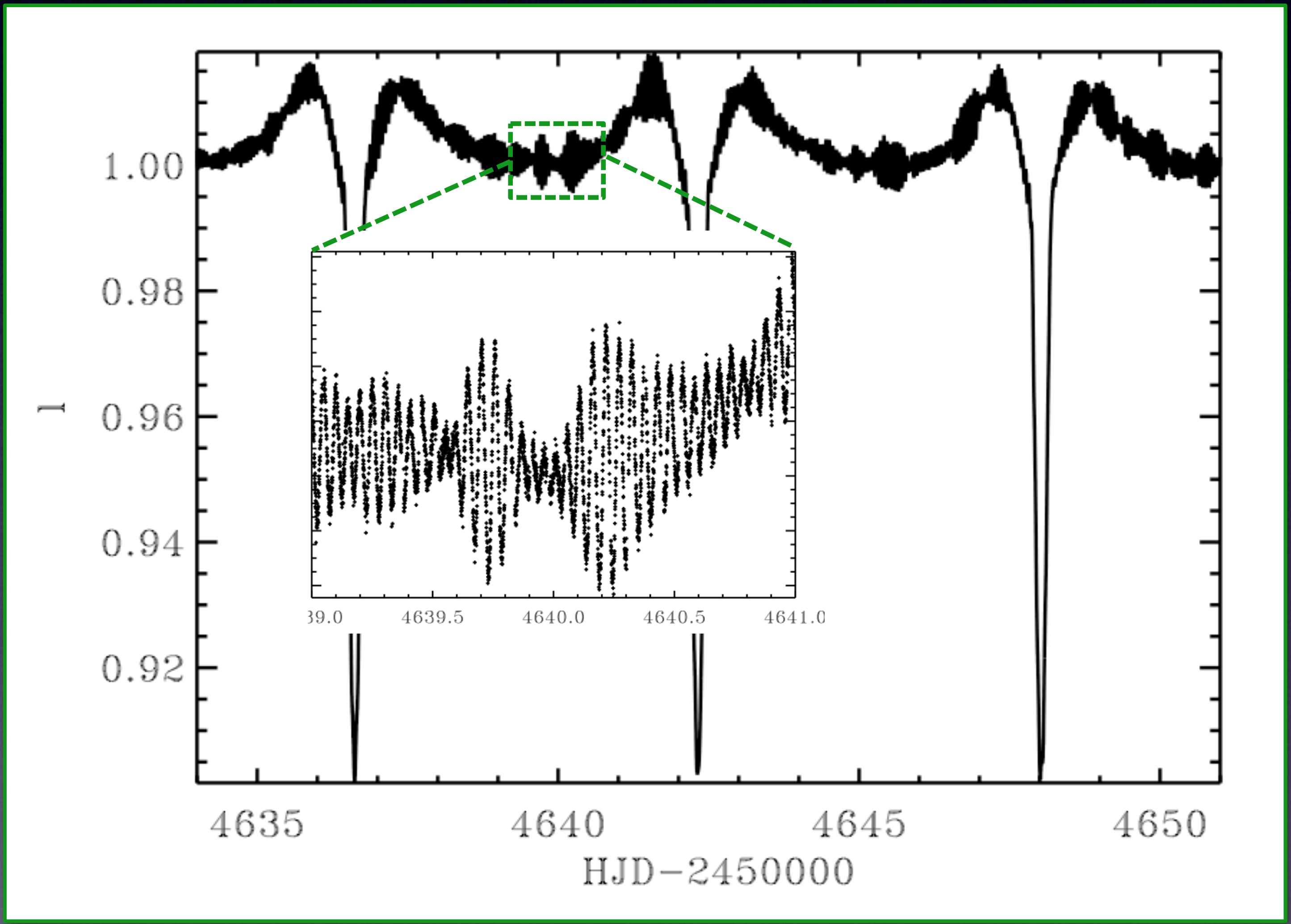

An enormous gain in terms of:
- number of observed points
- accuracy
- Monitoring interval & duty cycle

The pulsating EB zoo

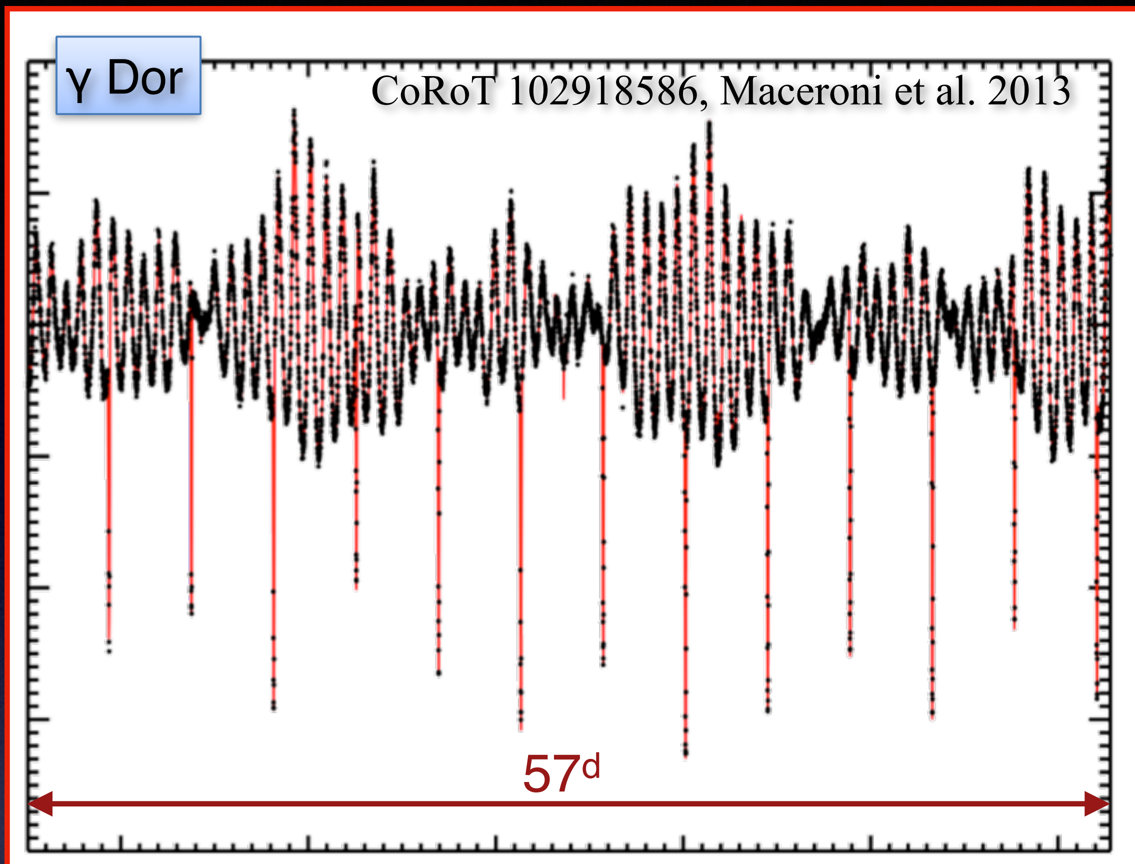

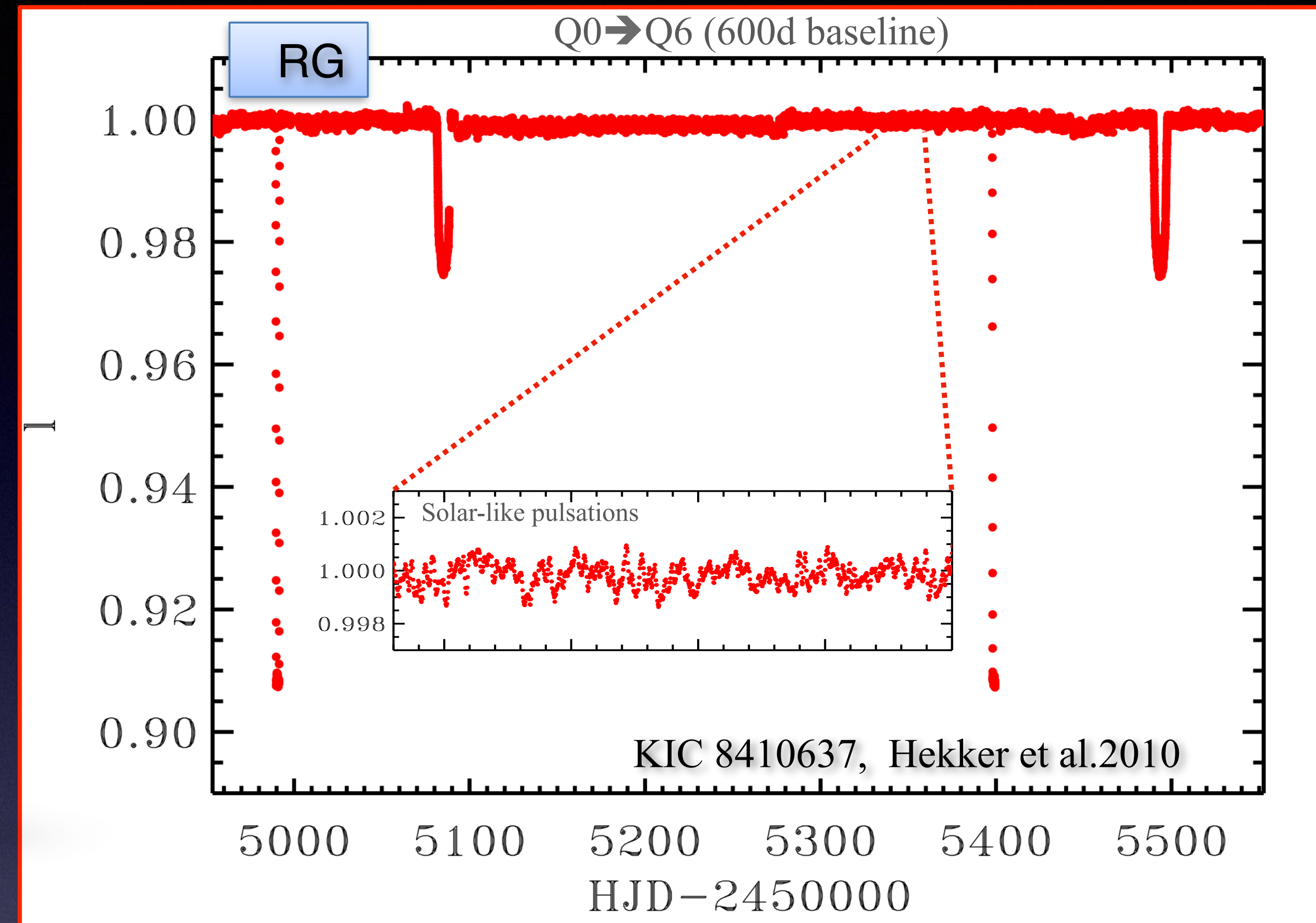

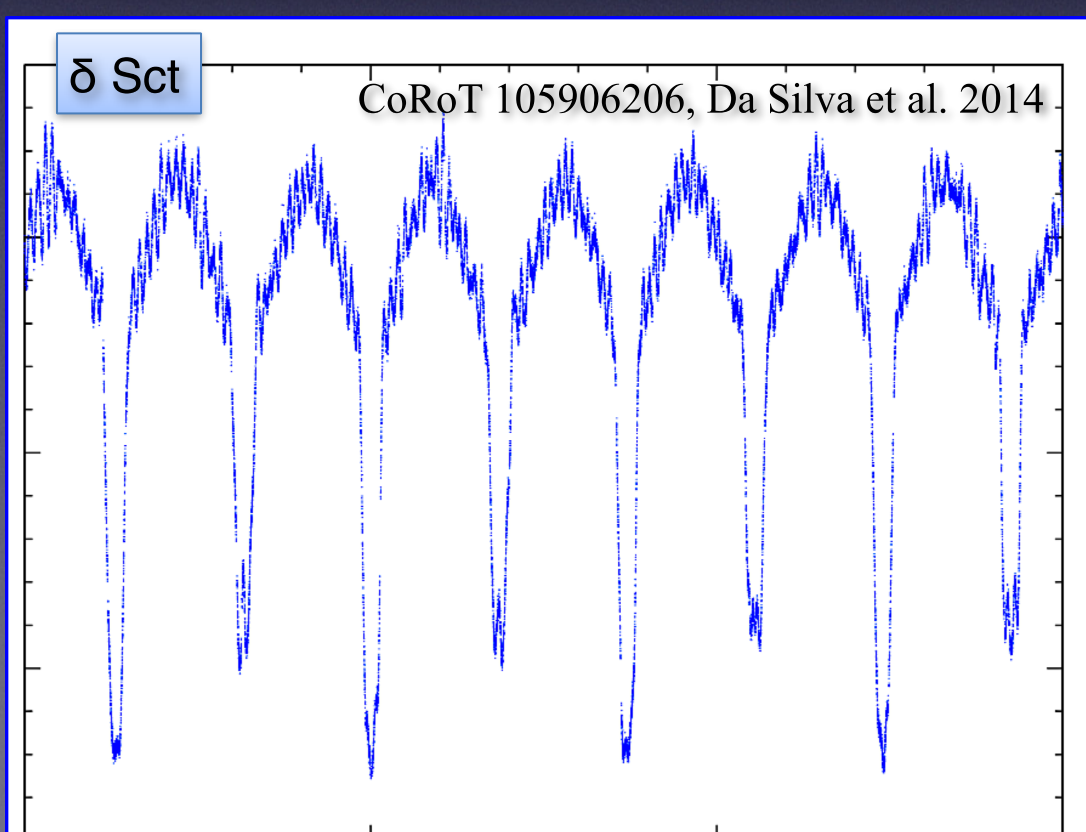

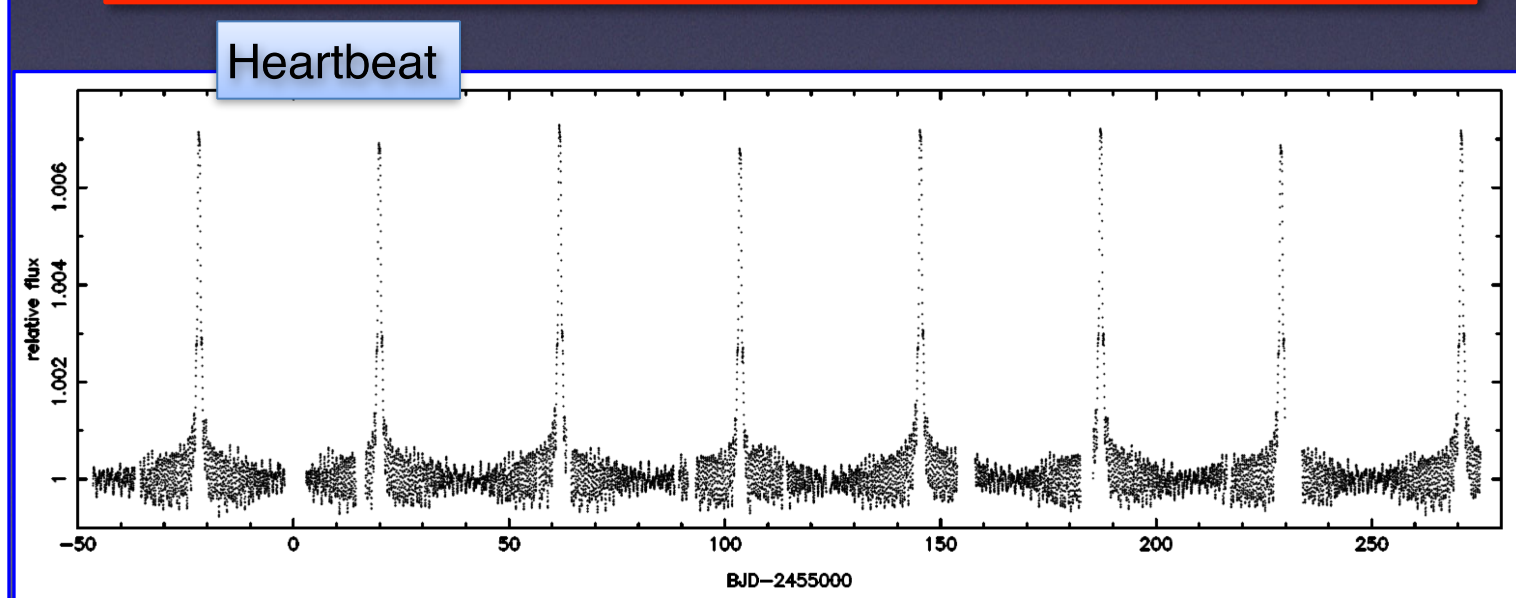

Tides in action! Brightening due to tidal distortion and irradiation at periastron. High order harmonics of F_{orb}

Iterative procedure

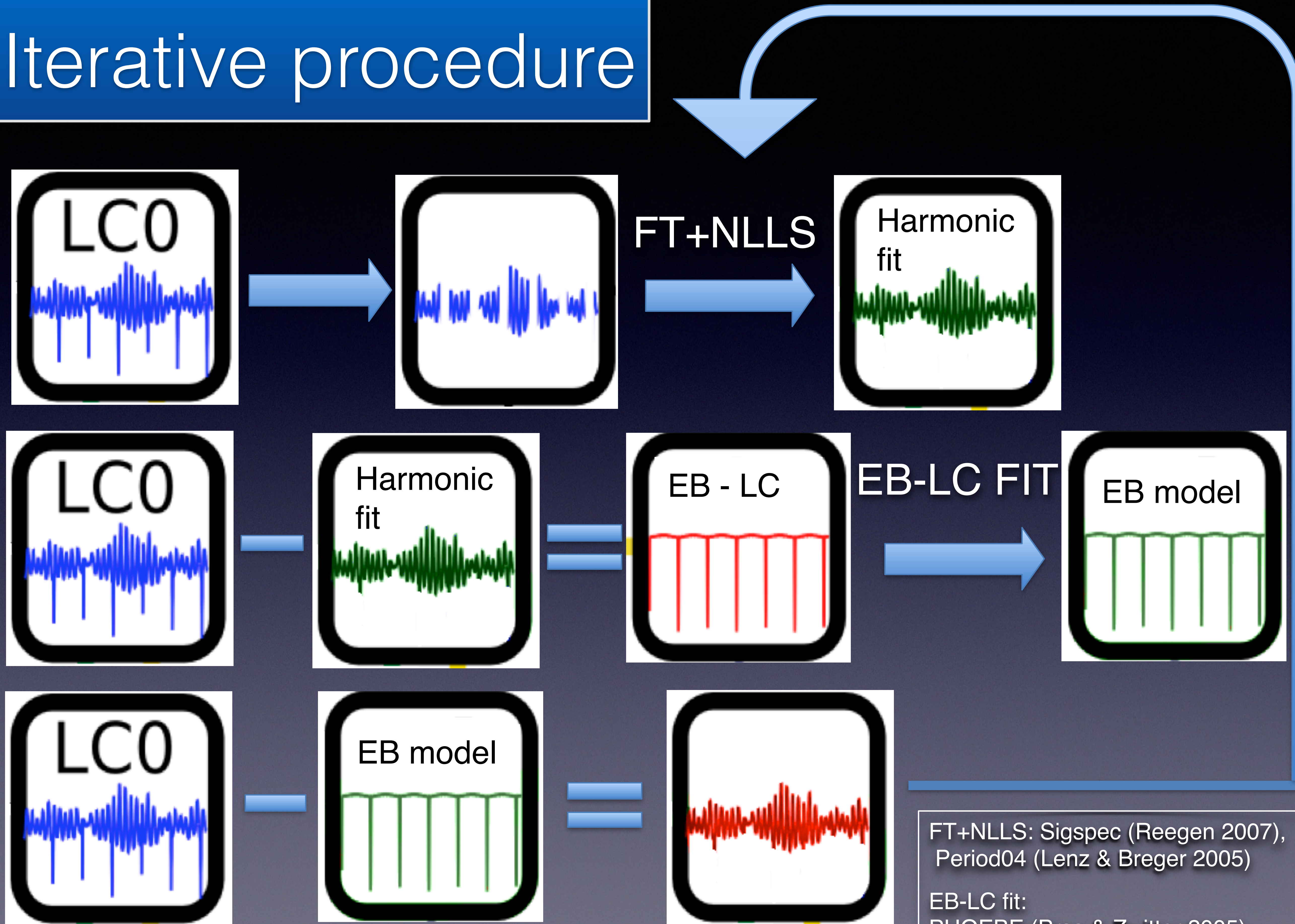

FT+NLLS: Sigspec (Reegen 2007), Period04 (Lenz & Breger 2005)

EB-LC fit:
PHOEBE (Prsa & Zwitter 2005)
JKTEBOP (Southworth+ 2004)

KIC 3858884: a highly eccentric eclipsing binary & δ Sct pulsator

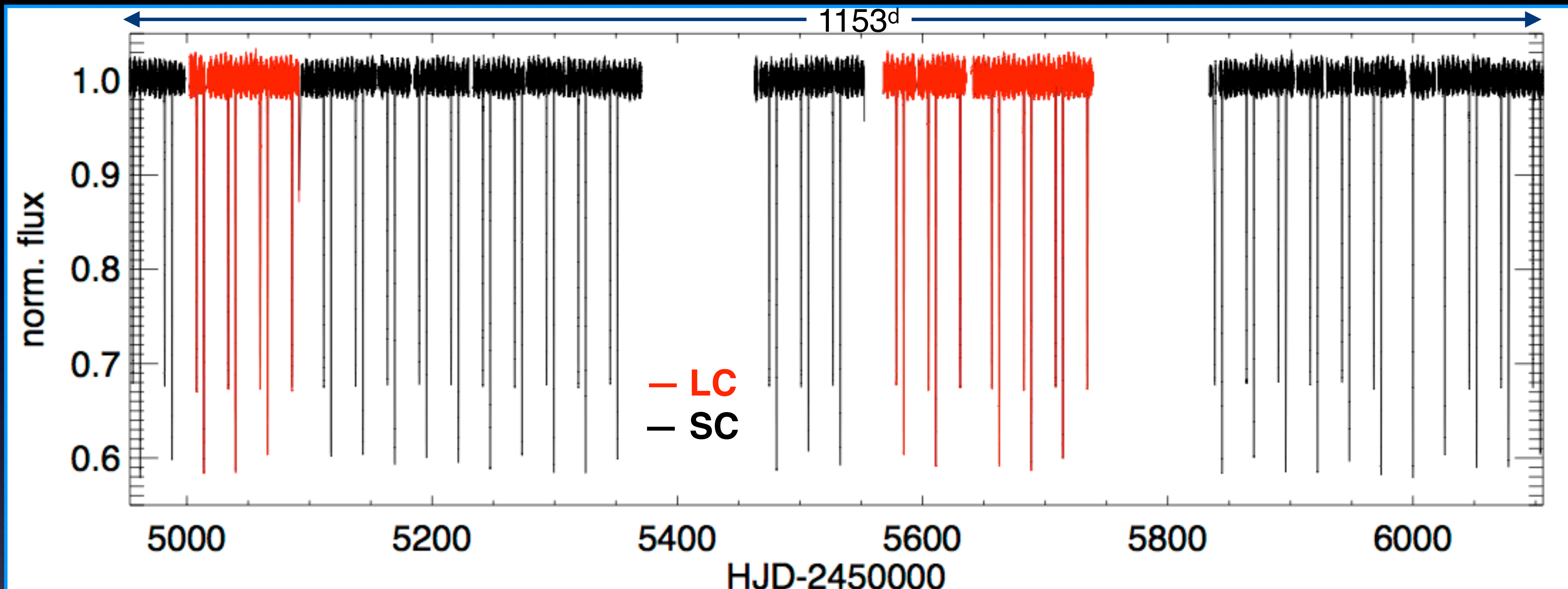

KIC 3858884: a highly eccentric eclipsing binary & δ Sct pulsator

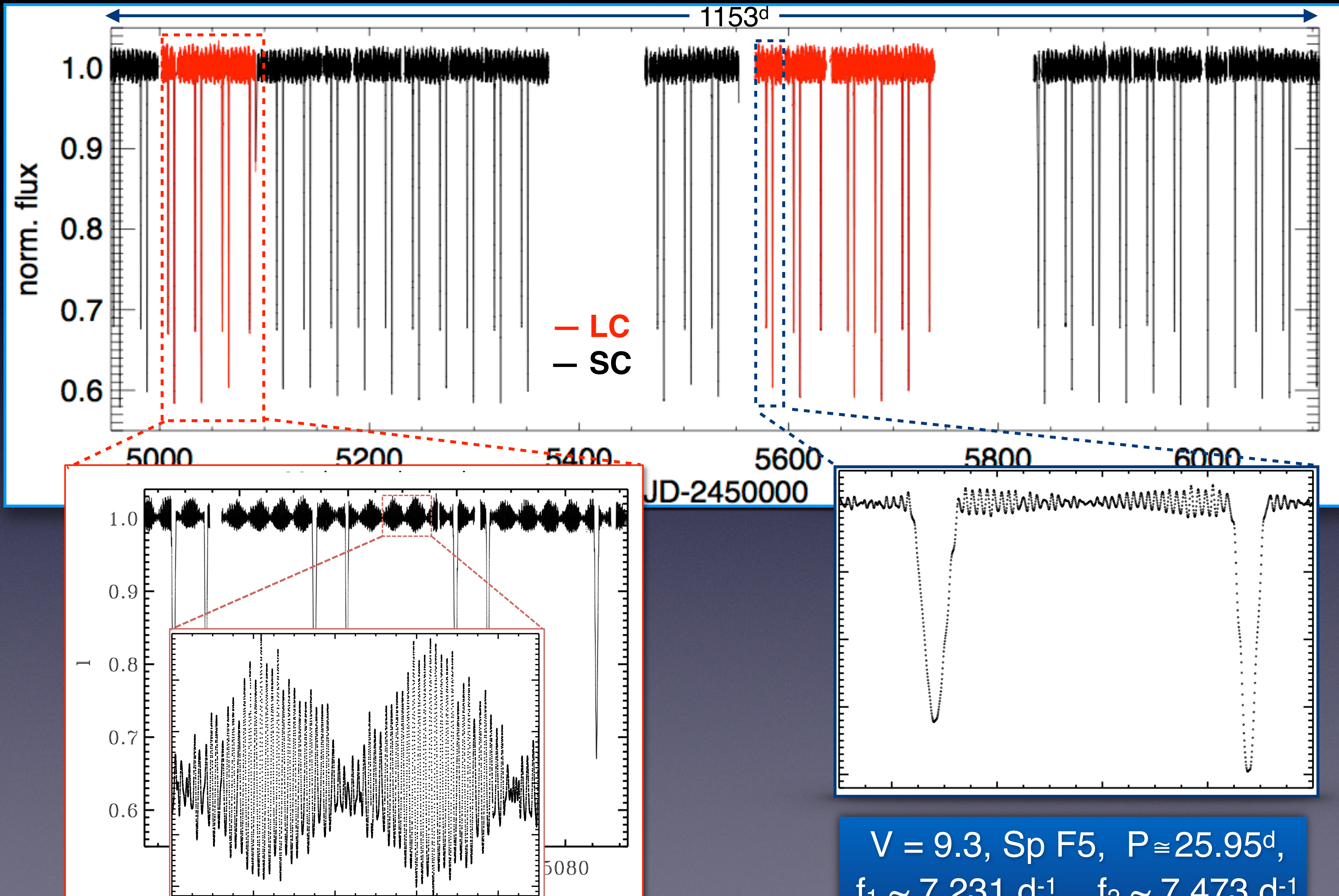

V = 9.3, Sp F5, $P \cong 25.95^d$,
$f_1 \sim 7.231\ d^{-1}$ $f_2 \sim 7.473\ d^{-1}$

Disentangling EB and pulsations

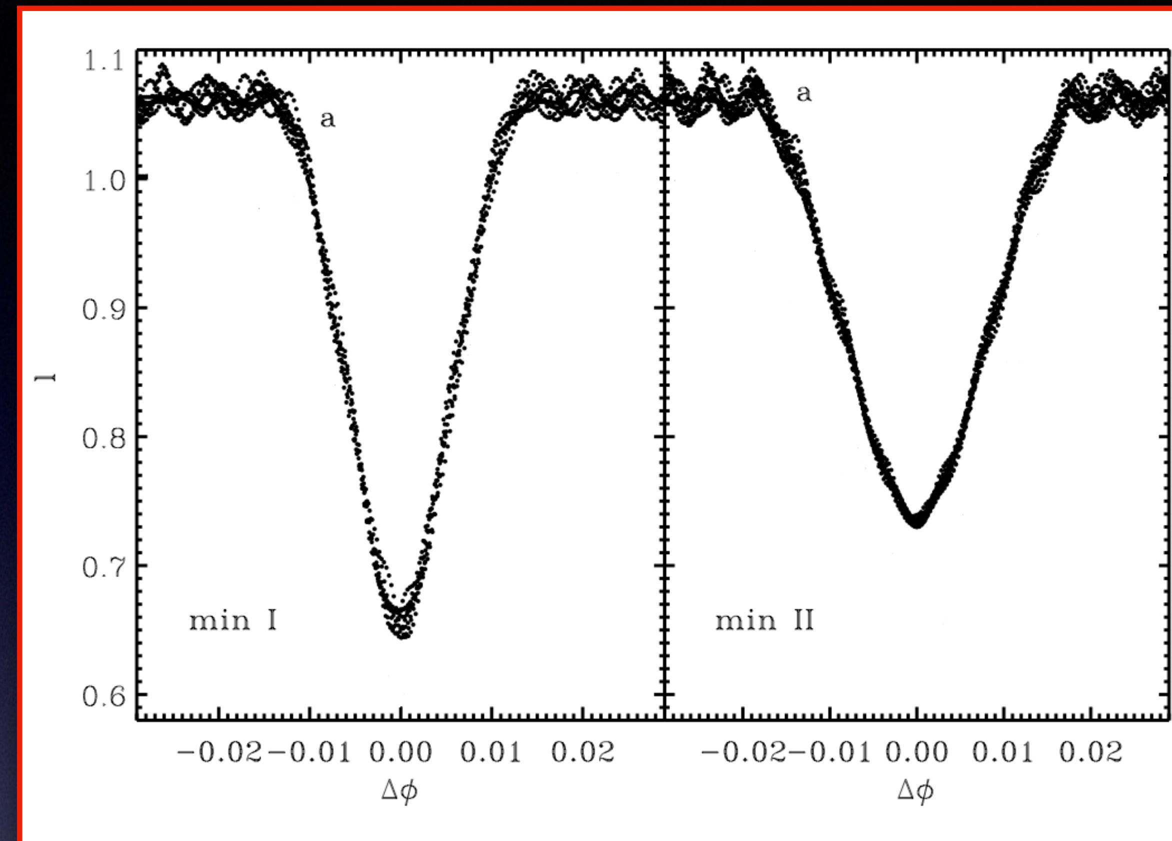

Disentangling EB and pulsations

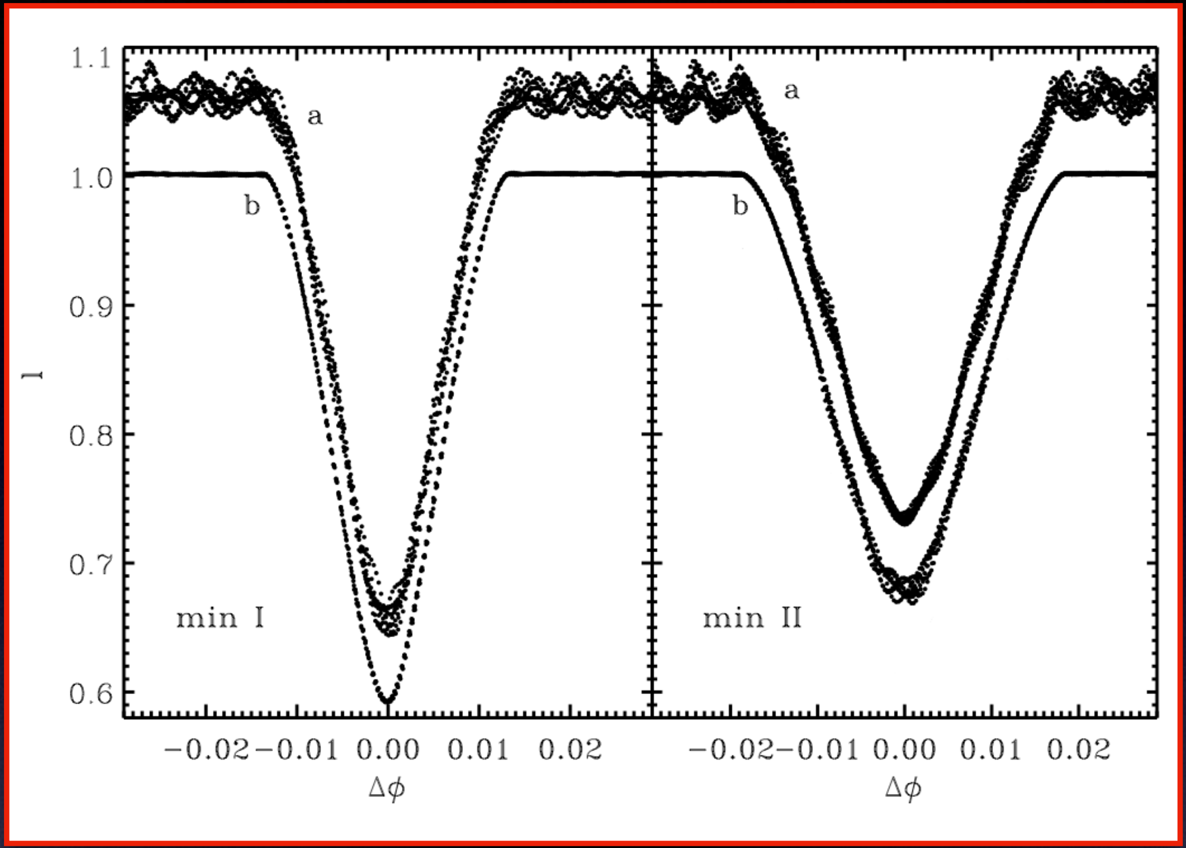

Disentangling EB and pulsations

Recipe for a successful disentangling:

- first order correction: during pulsator eclipse the pulsation amplitude is weighted with the fraction of light from the eclipsed star

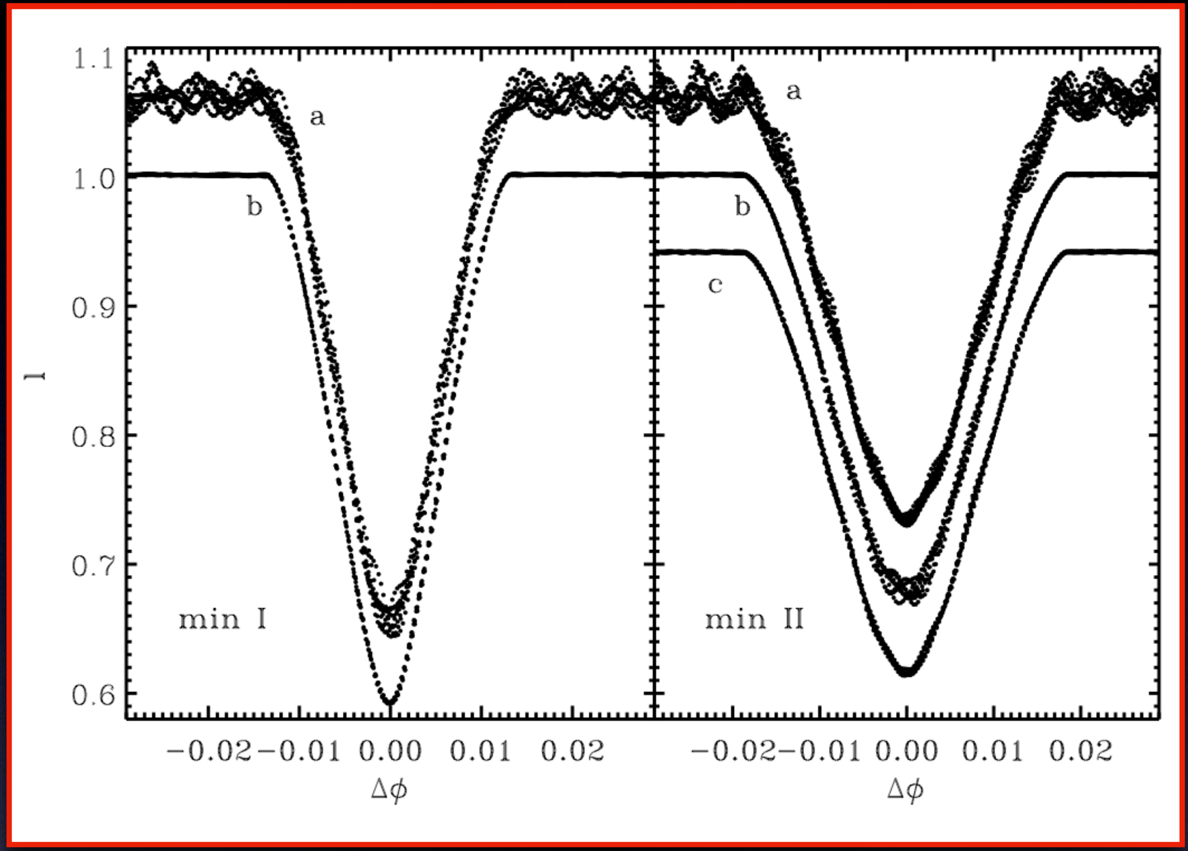

Disentangling EB and pulsations

Recipe for a successful disentangling:

- first order correction: during pulsator eclipse the pulsation amplitude is weighted with the fraction of light from the eclipsed star

- lower order orbital overtones (in this case up to ~ 15 f_{orb}) shall not be pre-whitened (due to eccentricity ‘bump”)

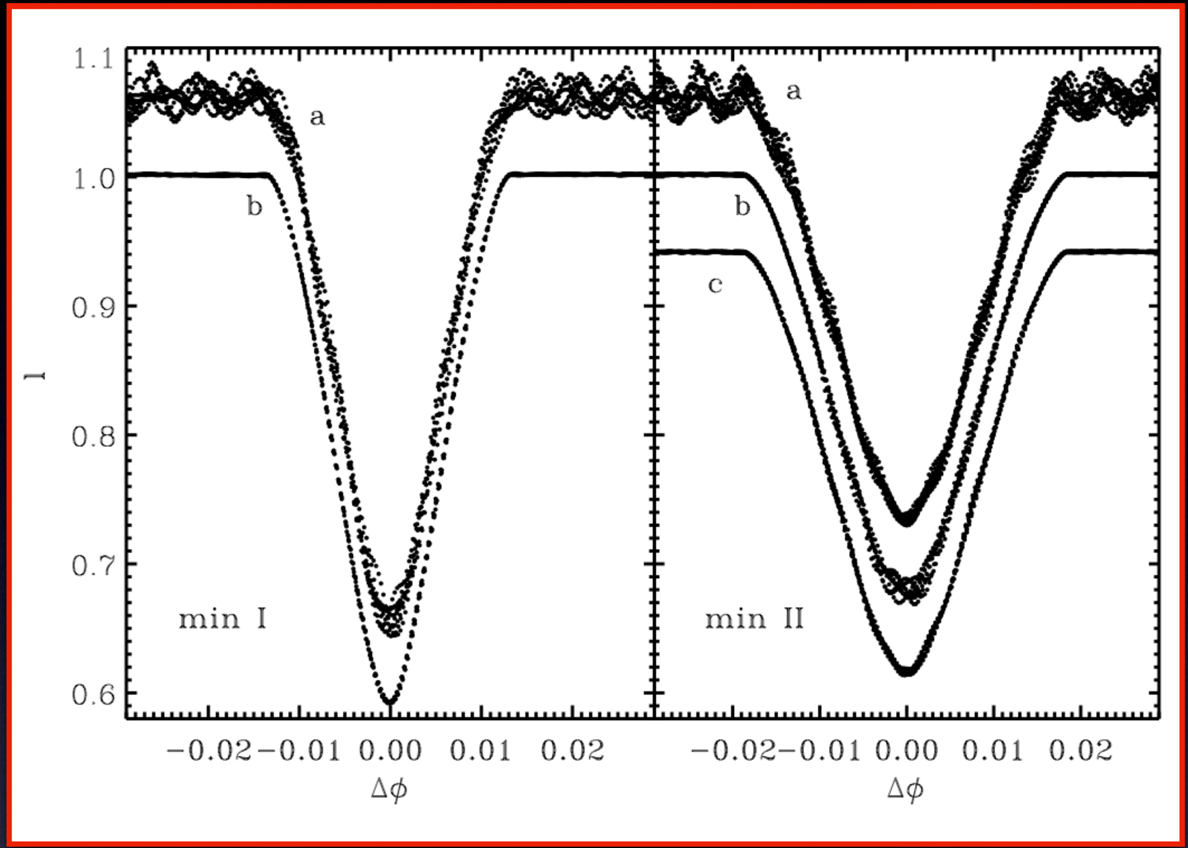

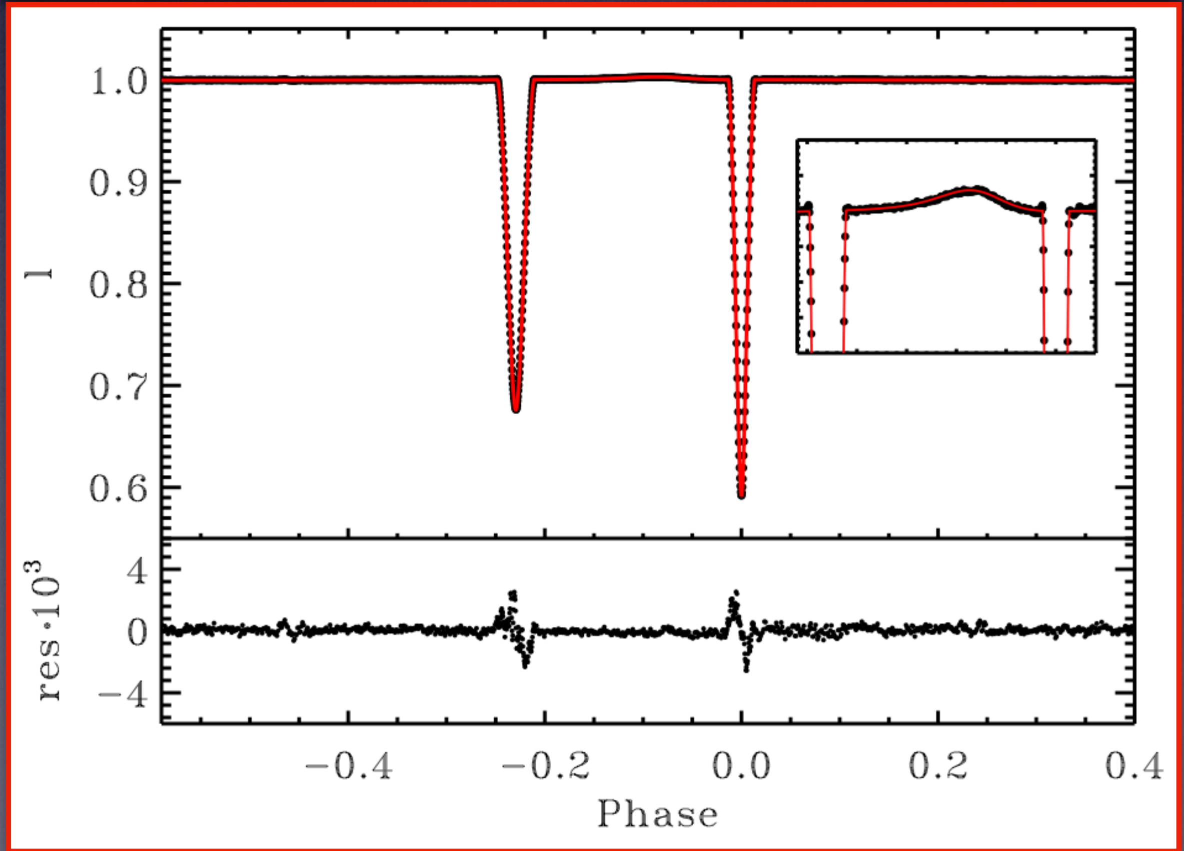

Radial velocity follow-up

83 high-res spectra (BOES, HRS, HERMES,TLS)
R=30000-83000

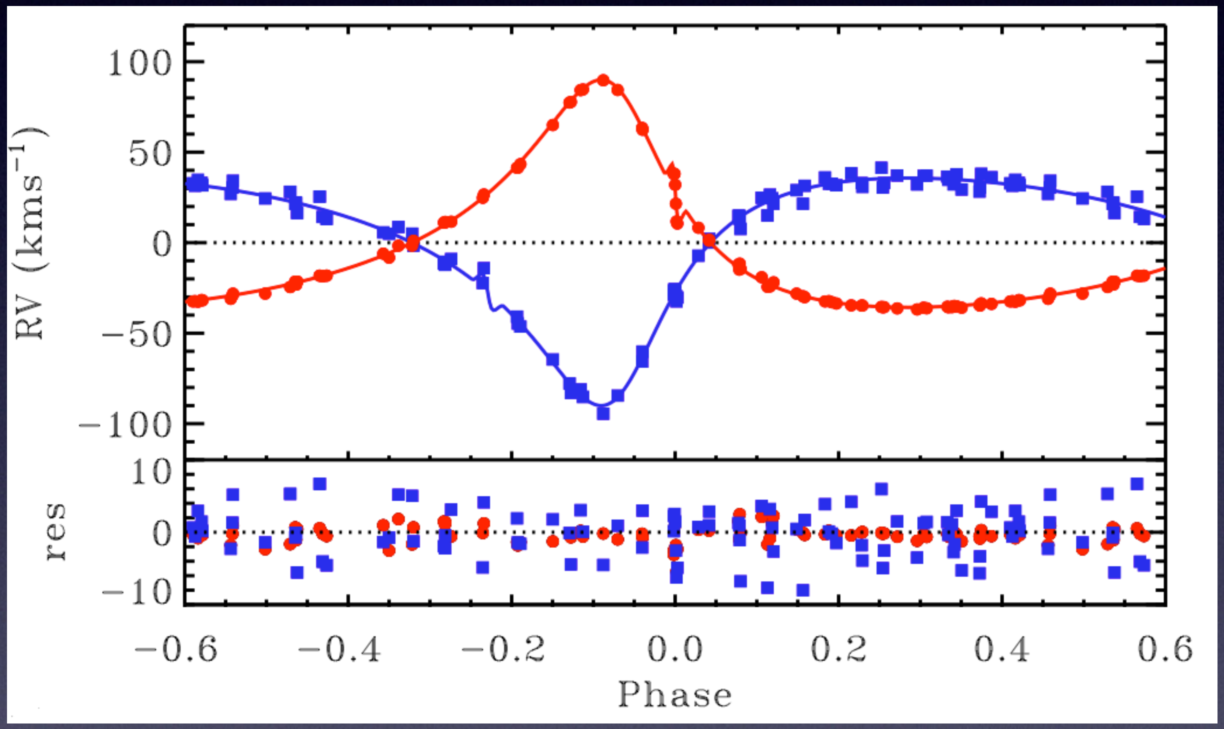

RVs
atmospheric
parameters

Radial velocity follow-up

83 high-res spectra (BOES, HRS, HERMES,TLS)
R=30000-83000

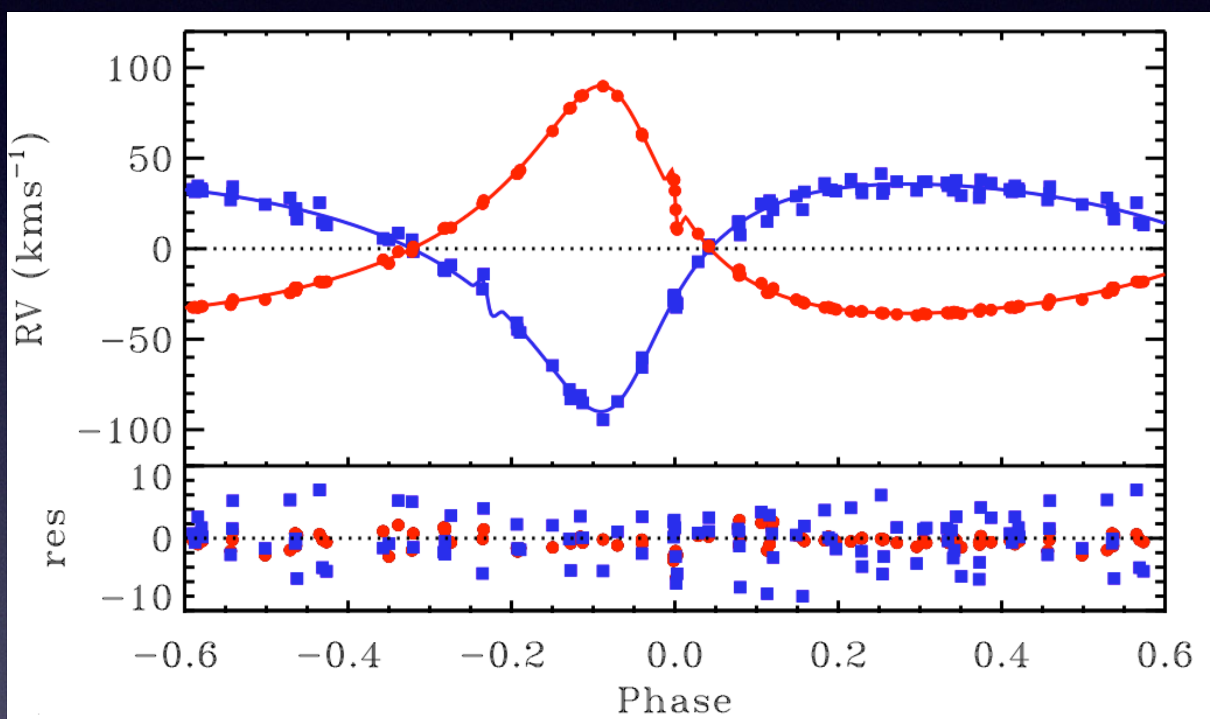

RVs
atmospheric
parameters

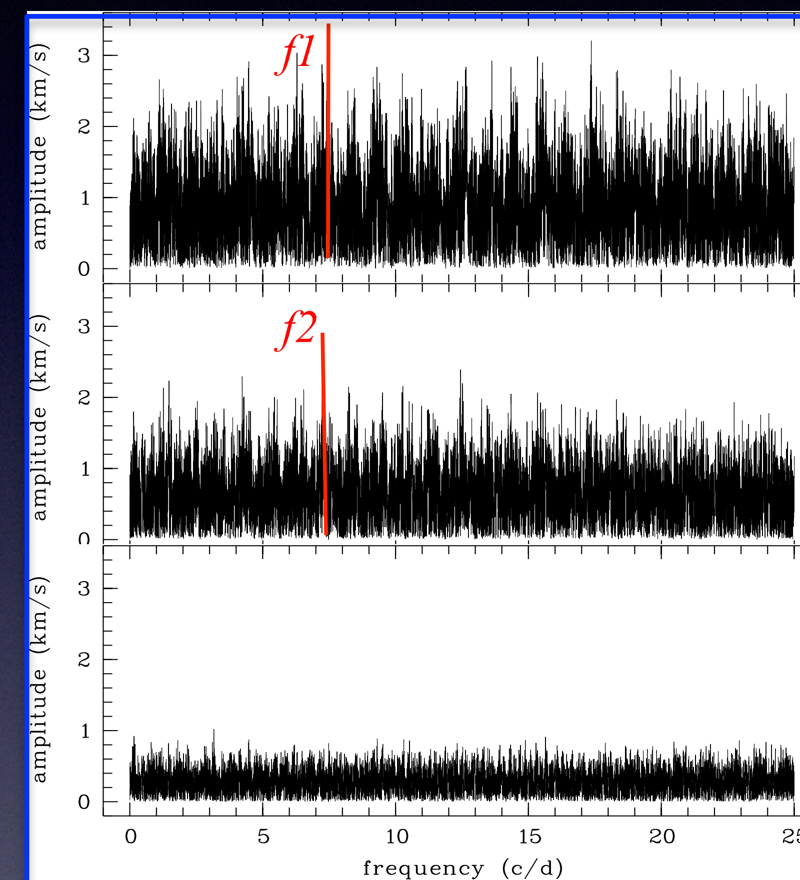

Photometry
$f_1 \sim 7.231$ d^{-1}
$f_2 \sim 7.473$ d^{-1}

Frequencies found in the O-C residuals

	f (d^{-1})	Ampl. (kms^{-1})	phase
$f1$	7.47927(20)	3.03(24)	0.805(15)
$f2$	7.23012(25)	2.80(25)	0.600(15)

Radial velocity follow-up

83 high-res spectra (BOES, HRS, HERMES,TLS)
R=30000-83000

RVs
atmospheric
parameters

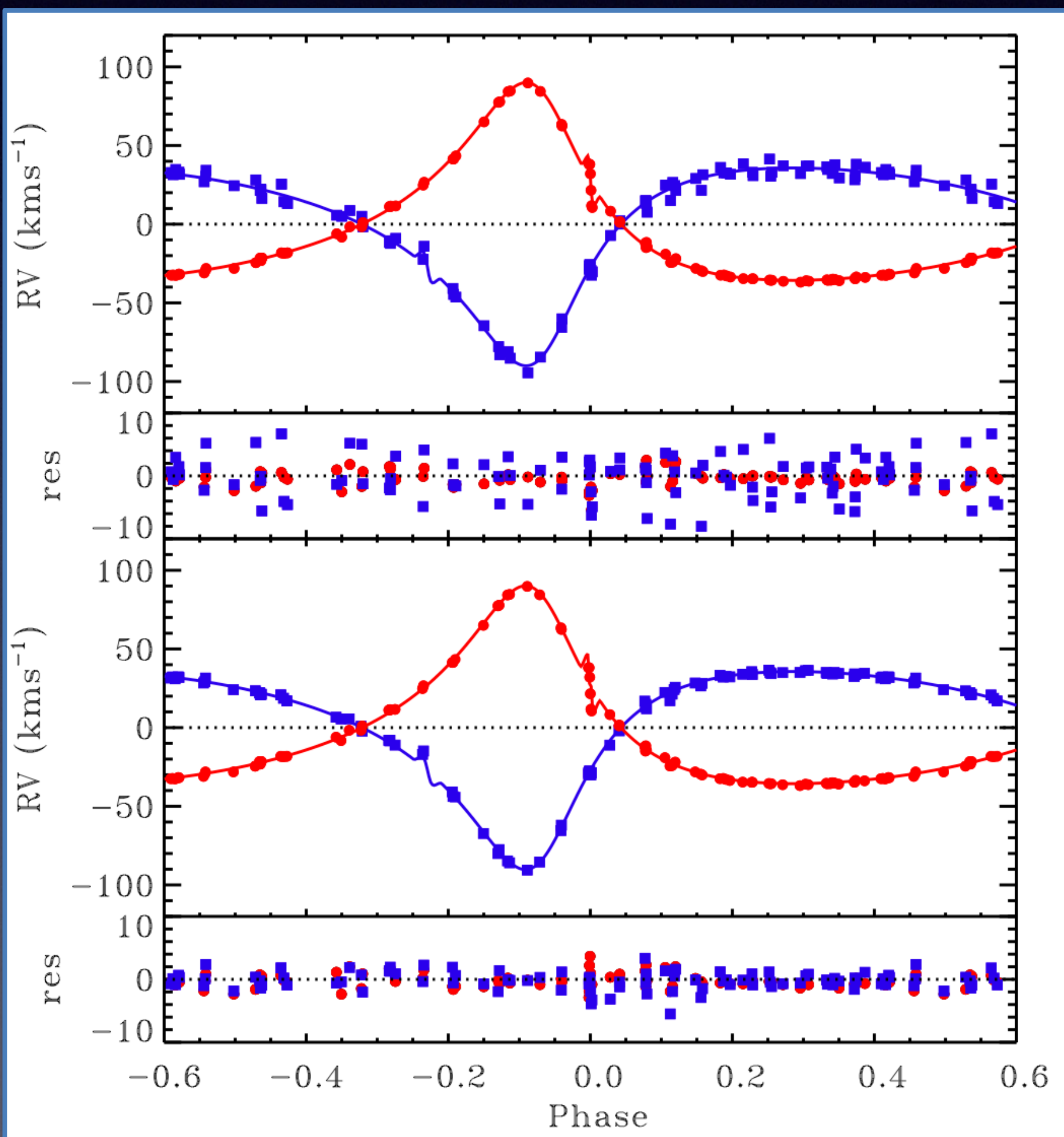

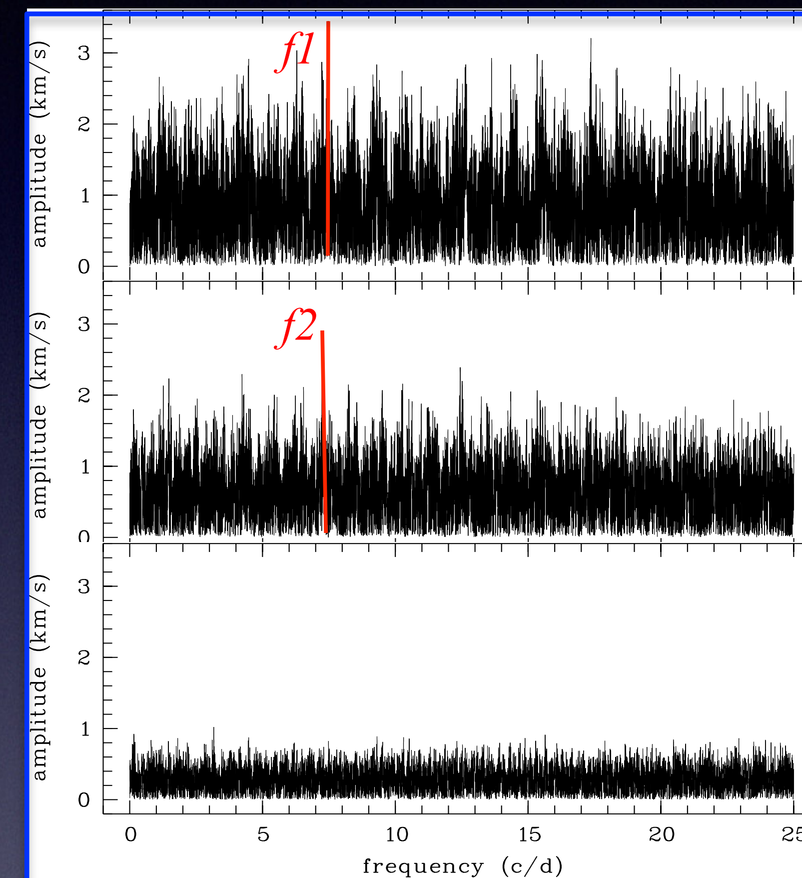

Photometry
$f_1 \sim 7.231\ d^{-1}$
$f_2 \sim 7.473\ d^{-1}$

Frequencies found in the O-C residuals

	f (d^{-1})	Ampl. (kms^{-1})	phase
$f1$	7.47927(20)	3.03(24)	0.805(15)
$f2$	7.23012(25)	2.80(25)	0.600(15)

Radial velocity follow-up

83 high-res spectra (BOES, HRS, HERMES,TLS)
R=30000-83000

RVs
atmospheric
parameters

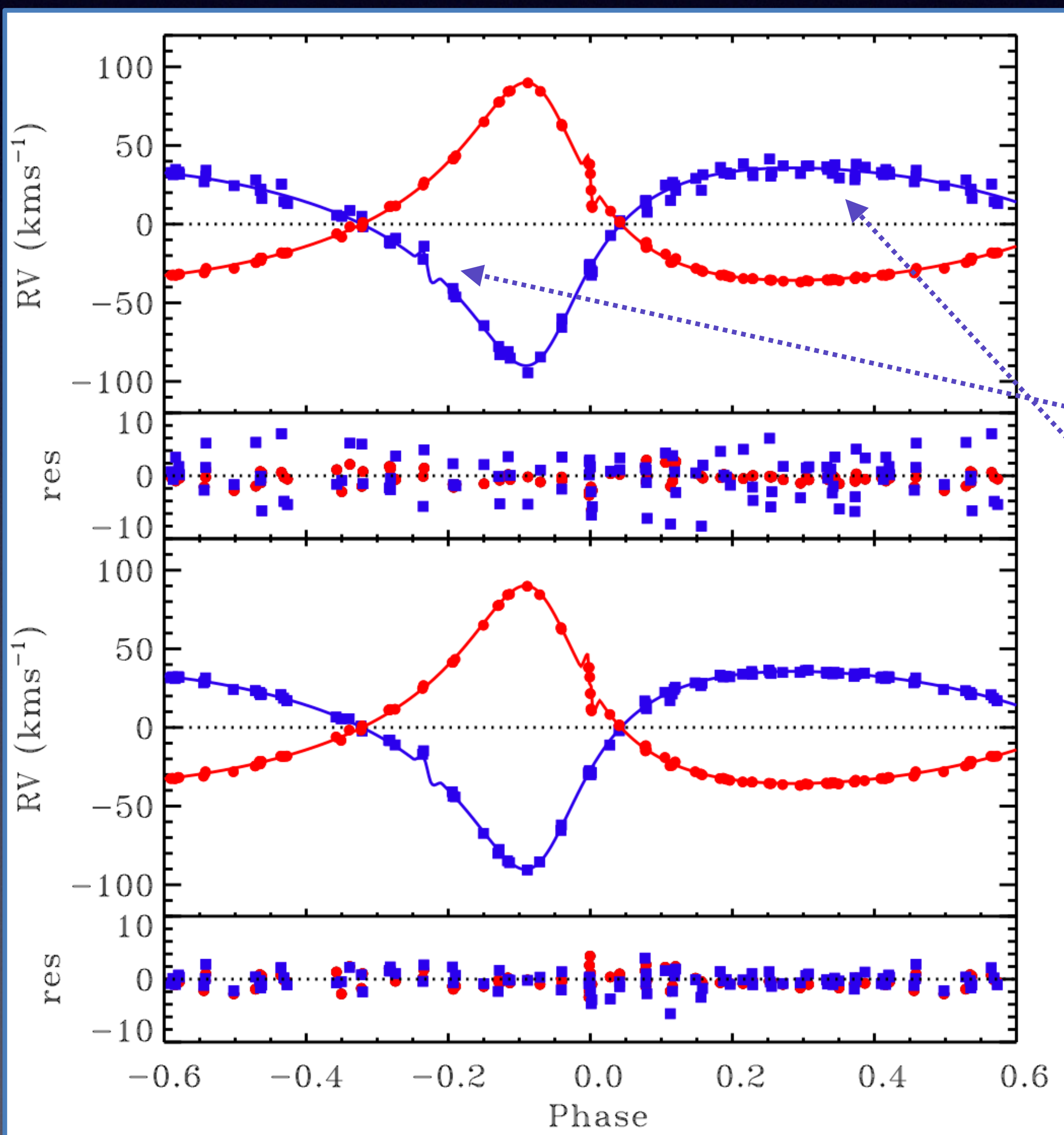

Rossiter effect
and
scatter due to
profile variation

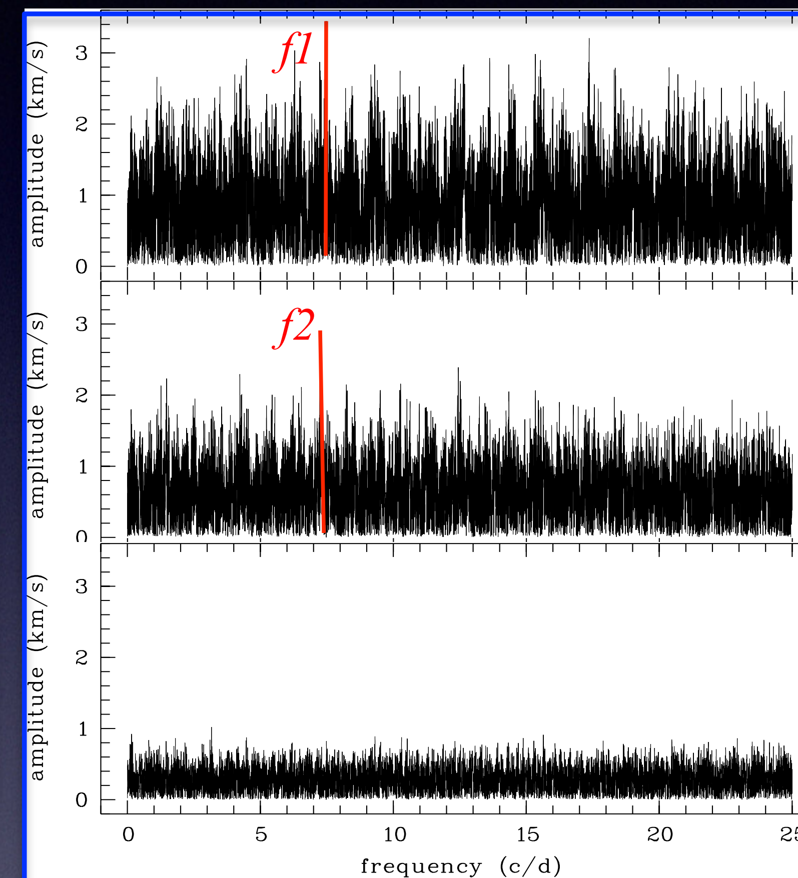

Photometry
$f_1 \sim 7.231$ d^{-1}
$f_2 \sim 7.473$ d^{-1}

Frequencies found in the O-C residuals

	f (d^{-1})	Ampl. (kms^{-1})	phase
$f1$	7.47927(20)	3.03(24)	0.805(15)
$f2$	7.23012(25)	2.80(25)	0.600(15)

Radial velocity follow-up

83 high-res spectra (BOES, HRS, HERMES,TLS)
R=30000-83000

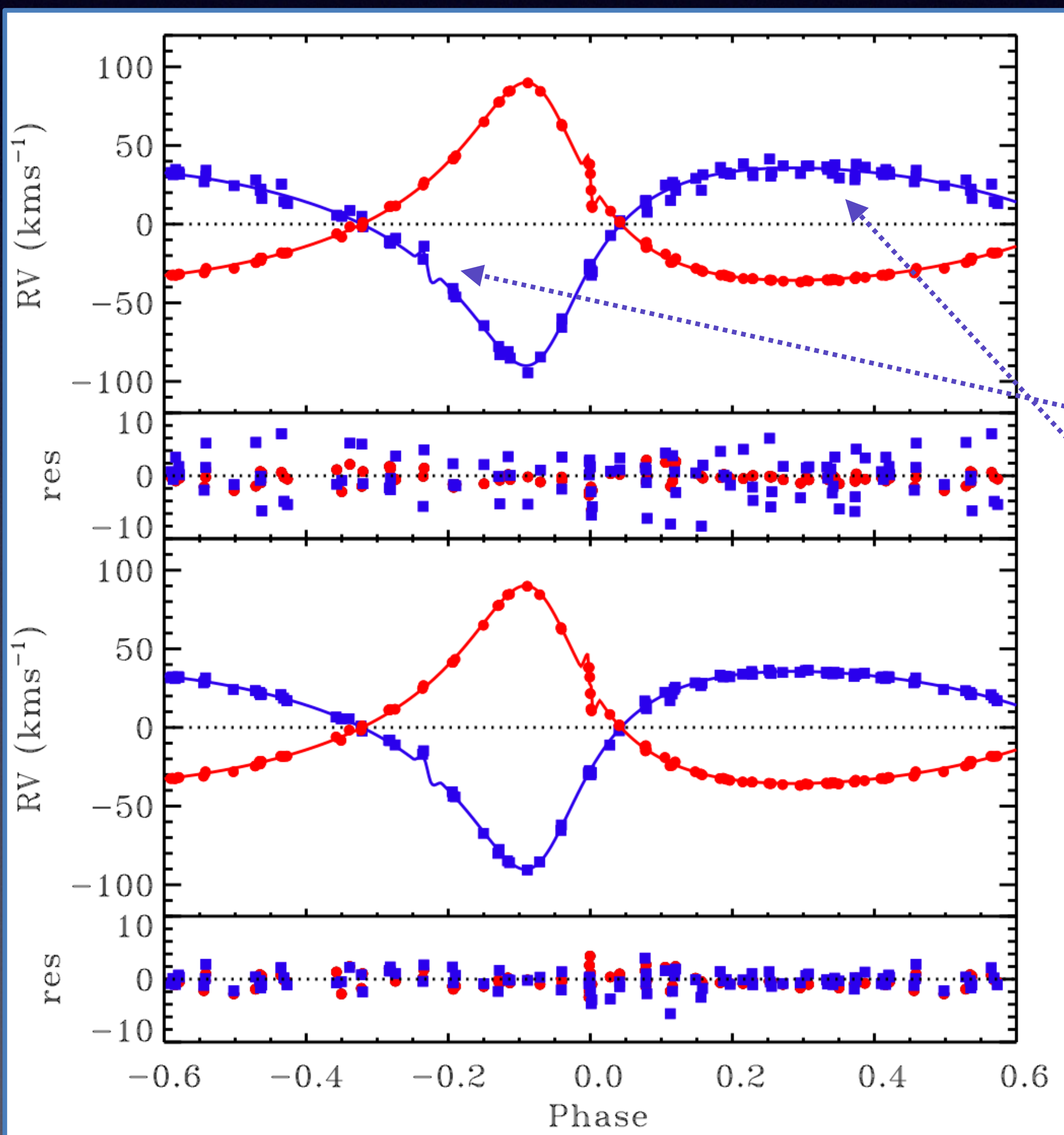

RVs
atmospheric
parameters

Rossiter effect
and
scatter due to
profile variation

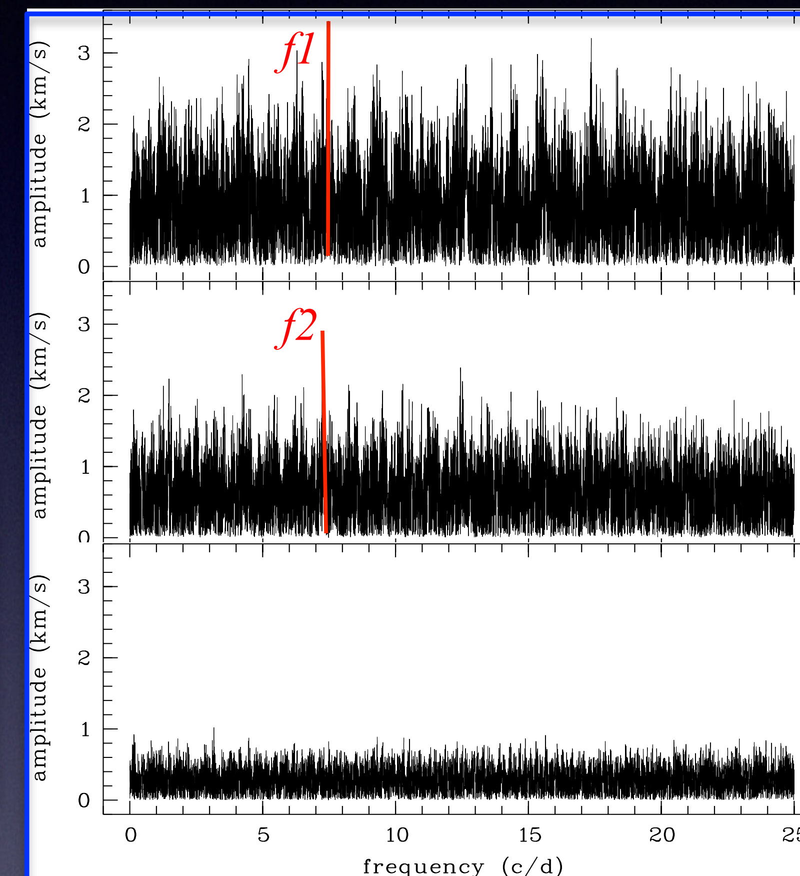

Photometry
$f_1 \sim 7.231\ d^{-1}$
$f_2 \sim 7.473\ d^{-1}$

Frequencies found in the O-C residuals

	f (d^{-1})	Ampl. (kms^{-1})	phase
$f1$	7.47927(20)	3.03(24)	0.805(15)
$f2$	7.23012(25)	2.80(25)	0.600(15)

the two largest amplitude frequencies
belong to the secondary star.

Physical parameters

Light and radial velocity curve solution: with FITBINARY (PHOEBE-WD + a genetic algorithm, PIKAIA, for global minimum search)

	System	
i (°)	88.176 ± 0.002	
e	0.465 ± 0.002	
ω	$21.61° \pm 0.01$	
q	0.988 ± 0.02	
$a(R_\odot)$	57.22 ± 0.22	
	Primary	**Secondary**
$T_{\rm eff}$ (K)	$6800^a \pm 70$	6606 ± 70
$M(M_\odot)$	1.88 ± 0.03	1.86 ± 0.04
$R(R_\odot)$	3.45 ± 0.01	3.05 ± 0.01
$\log g$	3.63 ± 0.01	3.74 ± 0.01

a) Fixed value, $\pm 1\sigma$ from spectroscopic analysis.

High eccentricity

- similar masses
- different R, $T_{\rm eff}$

↓

slightly evolved primary

Pulsational analysis

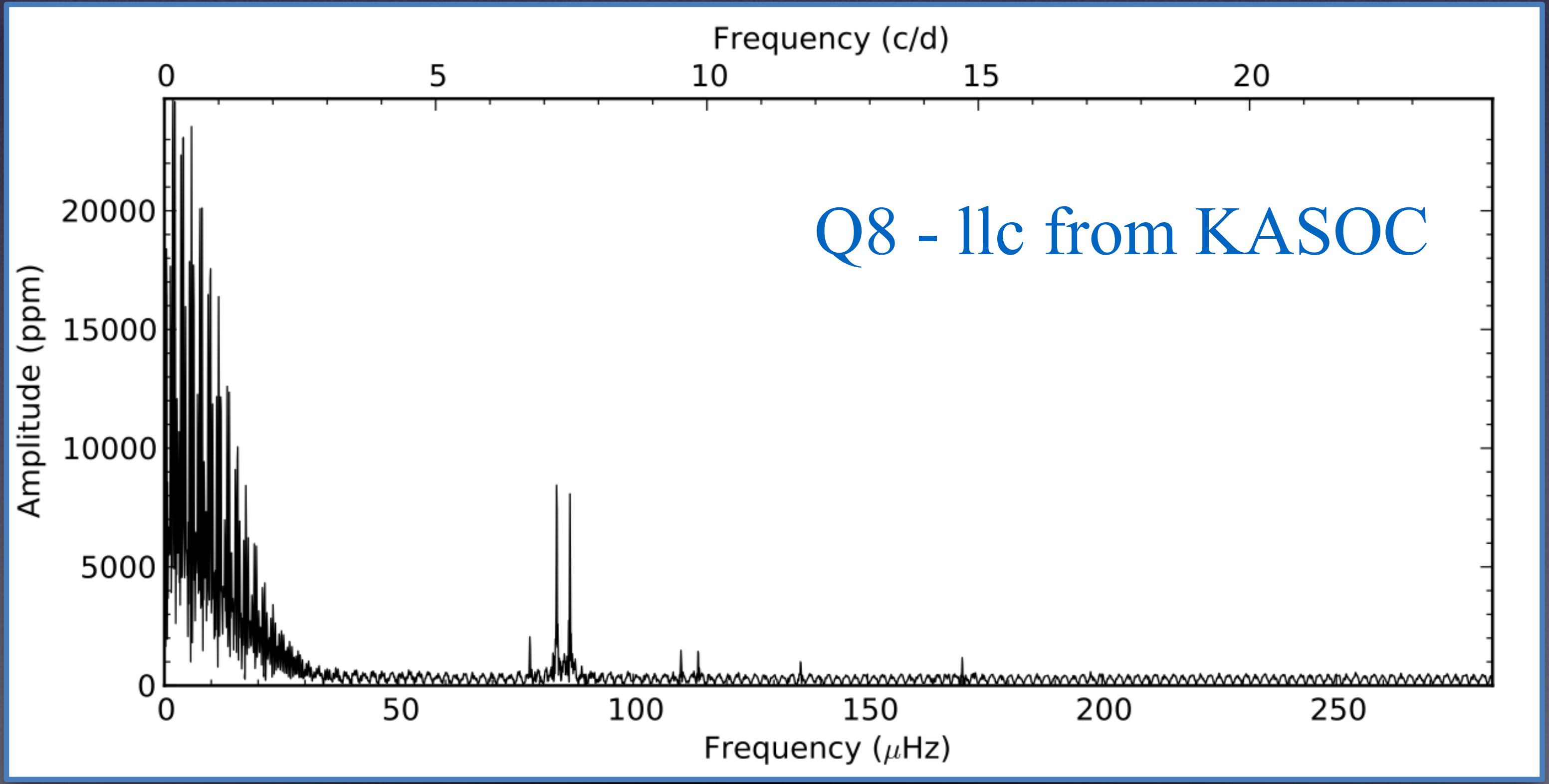

Pulsational analysis

after EB subtraction:
403 frequencies with
S/N > 4 (ξ < 12)
range: 0.3 - 20 d^{-1}
(Period04 and SigSpec)

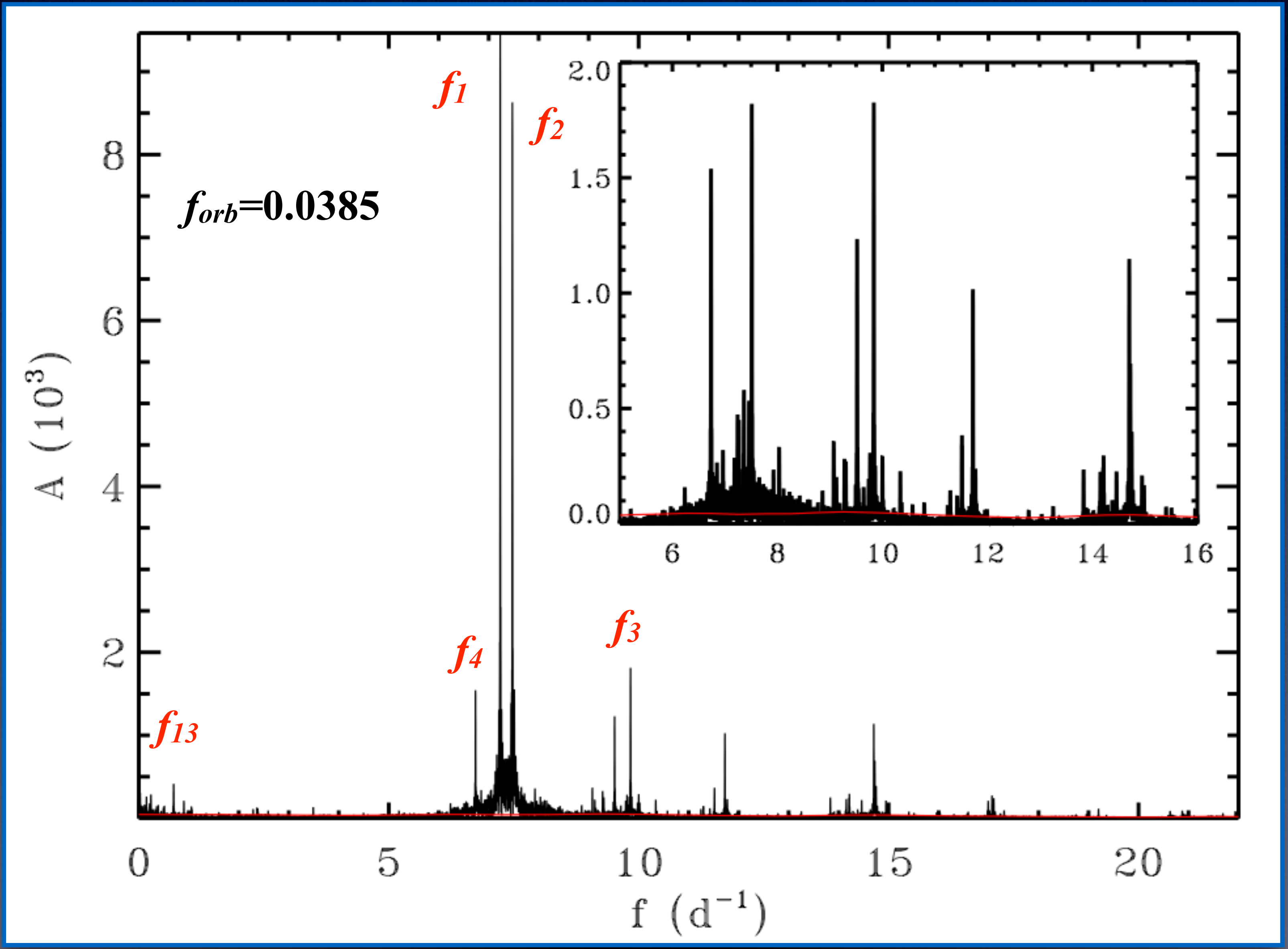

Pulsational analysis

	Frequency (d^{-1})	Amplitude (10^{-3})	Phase (2π)	remark
f_1	7.2306 ± 0.0001	10.15± 0.21	0.411 ± 0.002	
f_2	7.4734 ± 0.0001	9.10 ± 0.15	0.106 ± 0.001	
f_3	9.8376 ± 0.0002	1.96 ± 0.07	0.190 ± 0.002	
f_4	7.5125 ± 0.0002	1.75 ± 0.06	0.646 ± 0.002	$f_2 + f_{\rm orb}$
f_5	6.7358 ± 0.0002	1.55 ± 0.05	0.476 ± 0.002	
f_6	9.5191 ± 0.0002	1.24 ± 0.04	0.786 ± 0.003	
f_7	14.7041 ± 0.0002	1.15 ± 0.04	0.768 ± 0.002	$f_1 + f_2$
f_8	11.7257 ± 0.0002	1.02 ± 0.04	0.575 ± 0.003	
f_9	14.7253 ± 0.0003	0.59 ± 0.03	0.330 ± 0.004	
f_{10}	7.3628 ± 0.0003	0.54 ± 0.03	0.264 ± 0.004	
f_{11}	7.2424 ± 0.0004	0.51 ± 0.03	0.351 ± 0.005	
f_{12}	7.4621 ± 0.0004	0.50 ± 0.03	0.988 ± 0.005	
f_{13}	0.6971 ± 0.0004	0.38 ± 0.03	0.721 ± 0.005	$18 f_{\rm orb}$, gd
⋮				

after EB subtraction:
403 frequencies with
S/N > 4 (ξ < 12)
range: 0.3 - 20 d^{-1}
(Period04 and SigSpec)

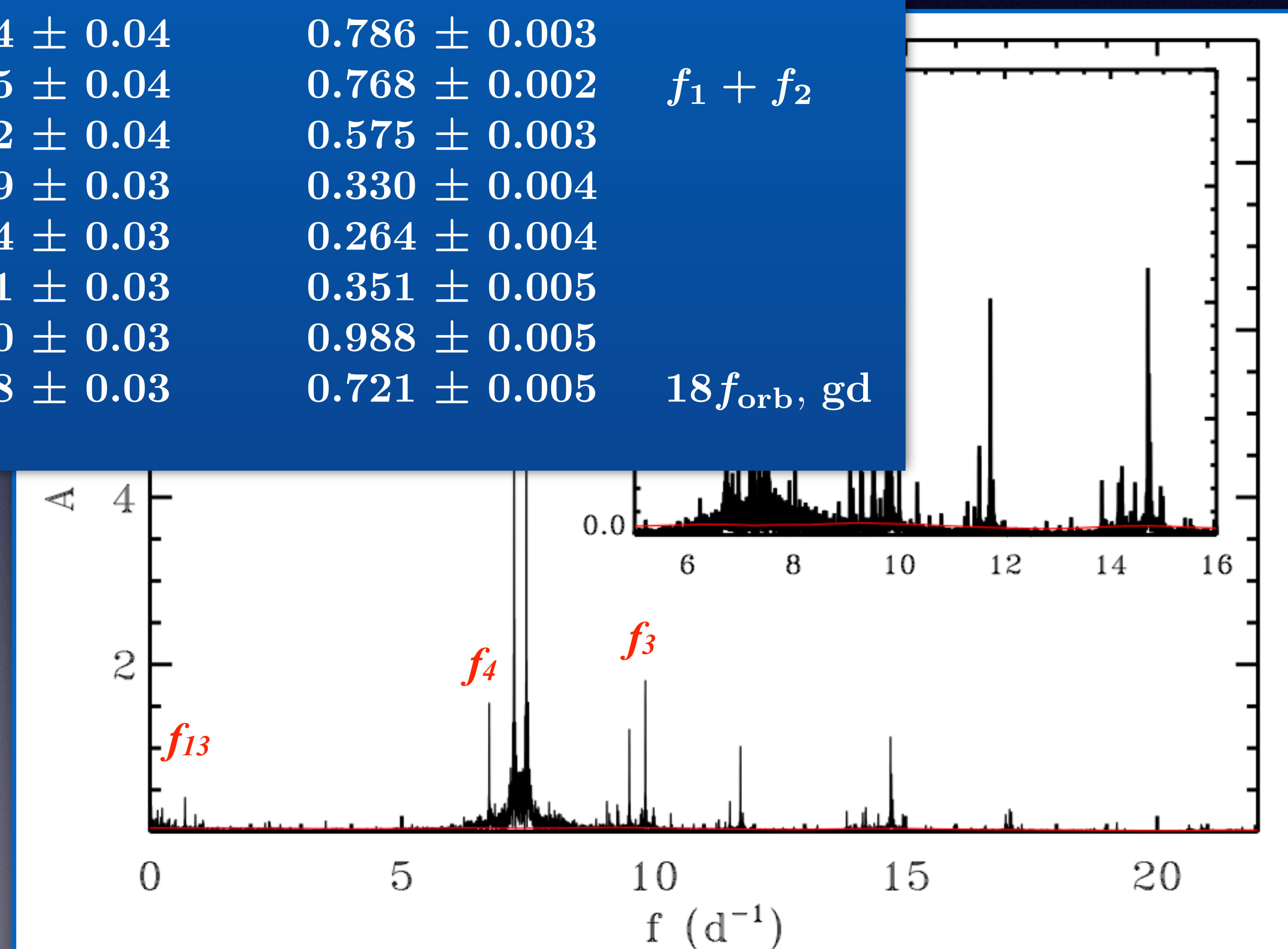

I. High frequency variability

Clustering of non-radial modes

(Dziembowski & Królikowska, 1990):

some low order ($l=1$) modes in δ Sct

- trapped in the envelope
- higher probability of excitation to observable amplitude
- close to radial mode frequency

⇒ clustering ⇒ preferred spacings

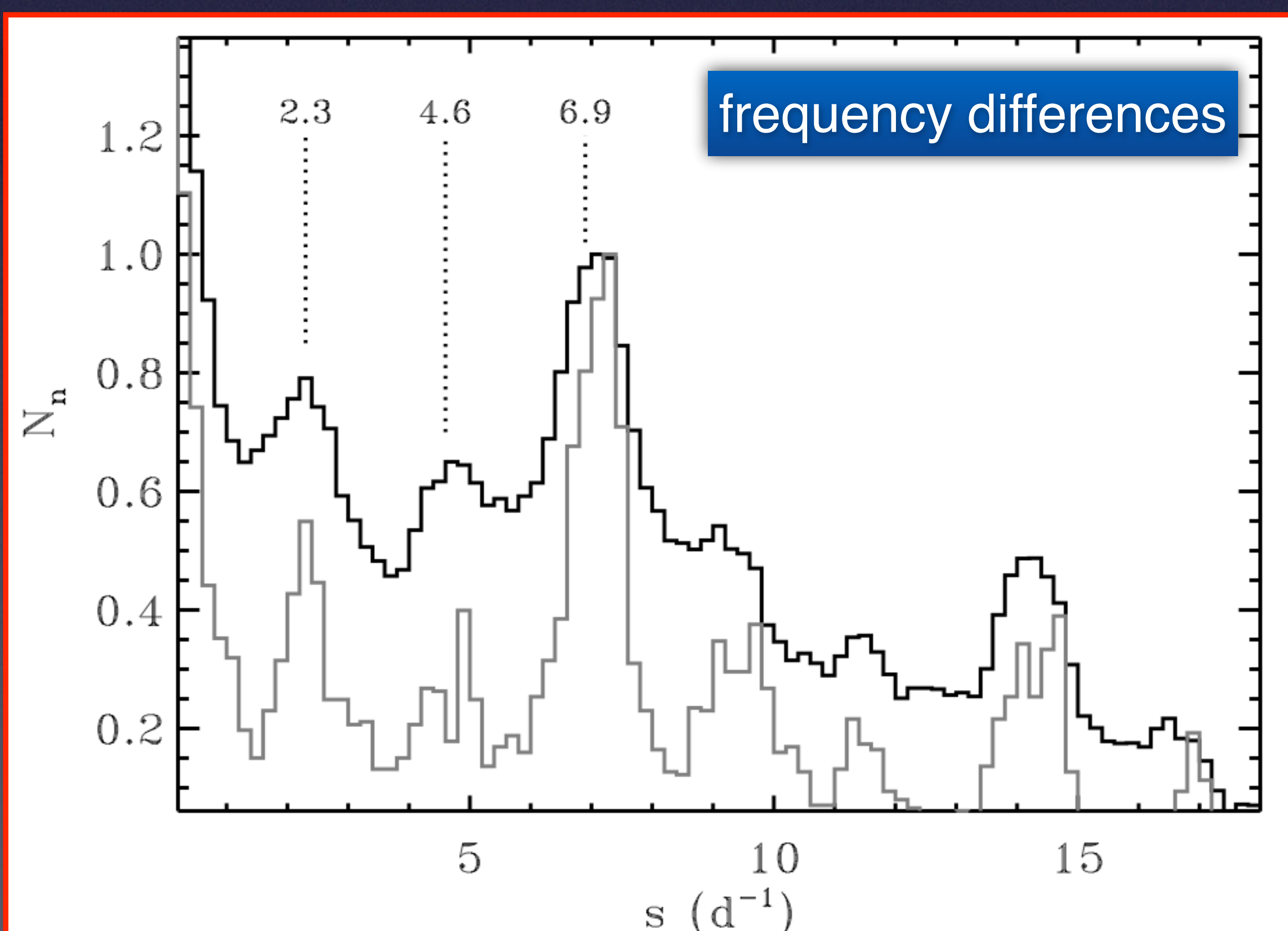

Breger et al. 2009, MNRAS 396, 291

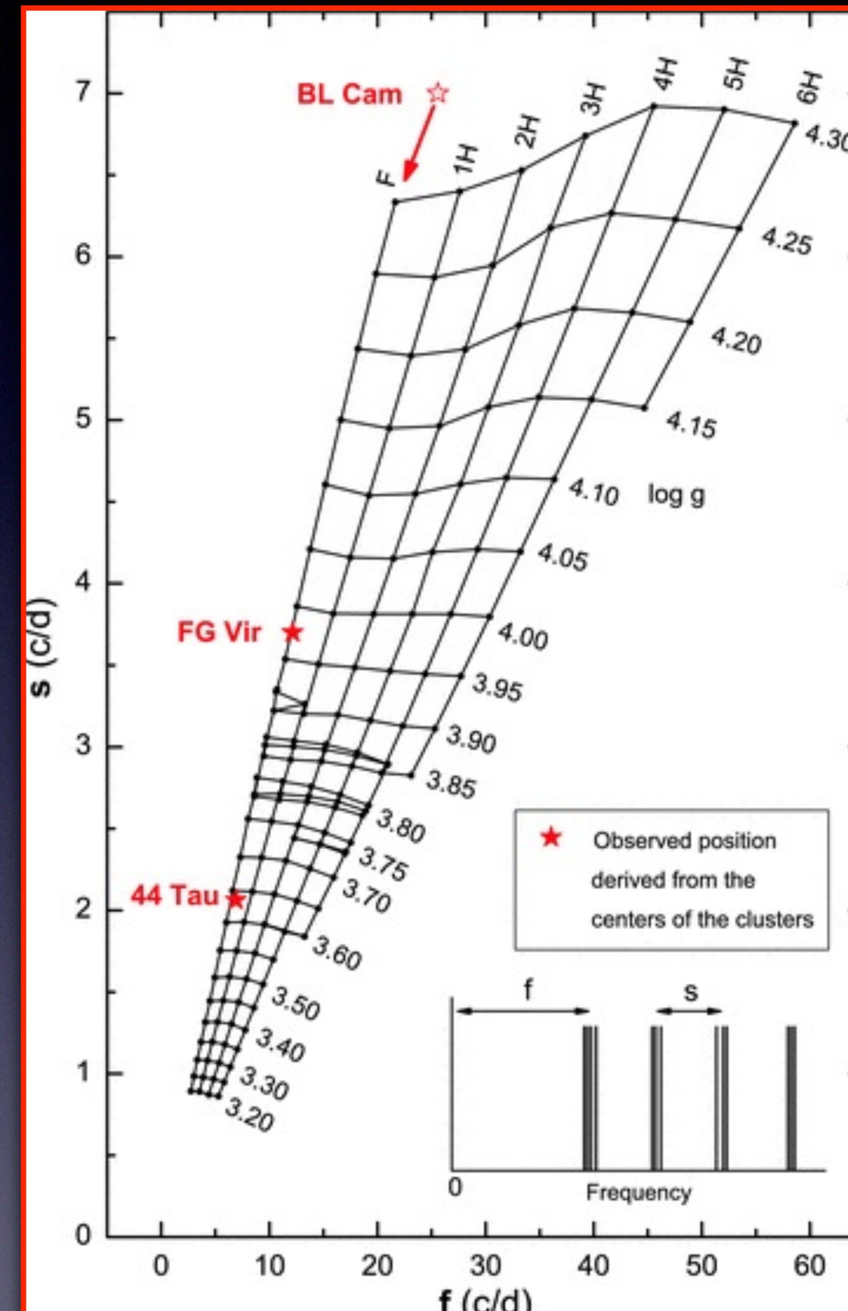

I. High frequency variability

Clustering of non-radial modes

(Dziembowski & Królikowska, 1990):

some low order (l=1) modes in δ Sct

- trapped in the envelope
- higher probability of excitation to observable amplitude
- close to radial mode frequency

⇒ clustering ⇒ preferred spacings

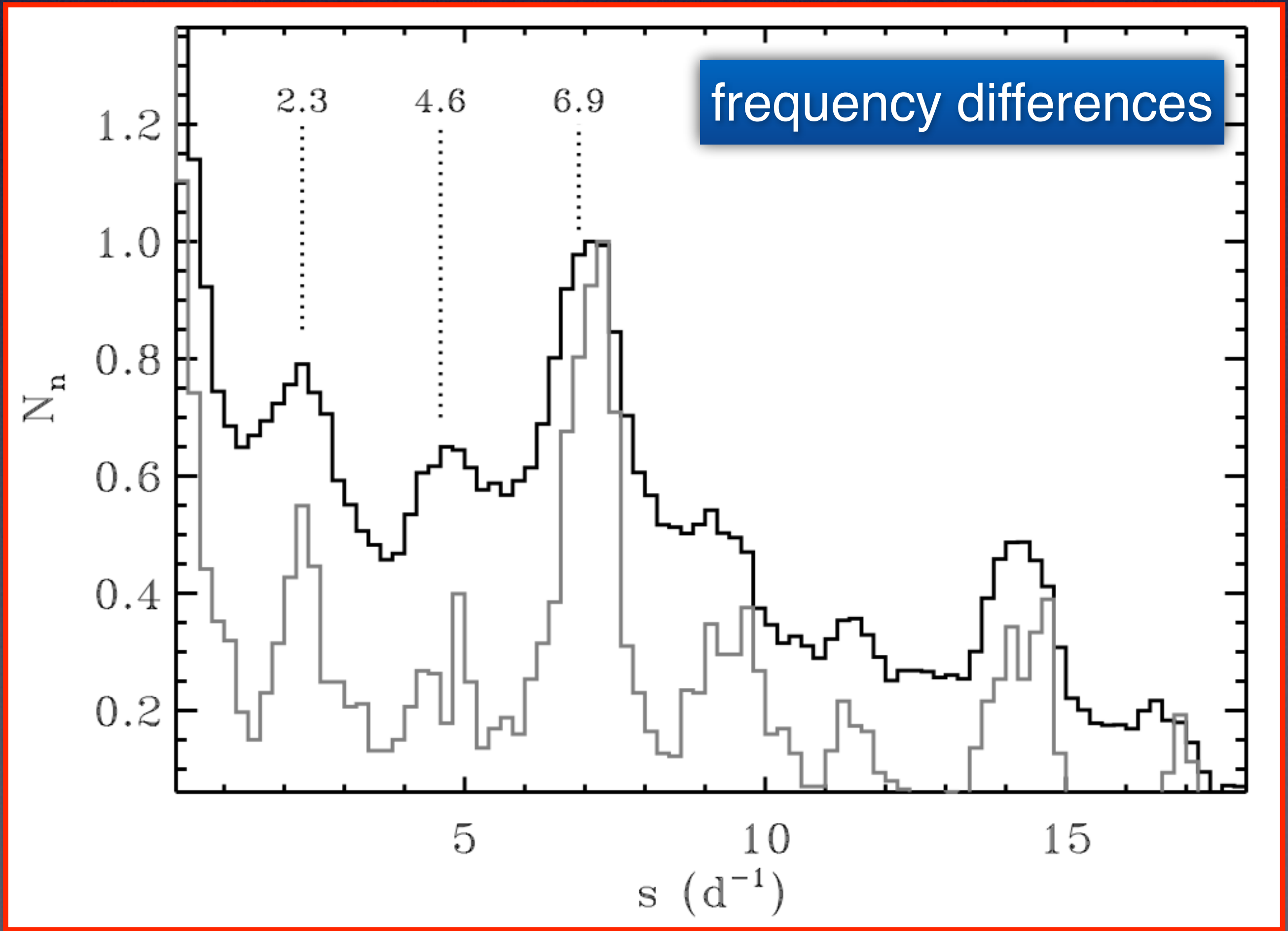

Breger et al. 2009, MNRAS 396, 291

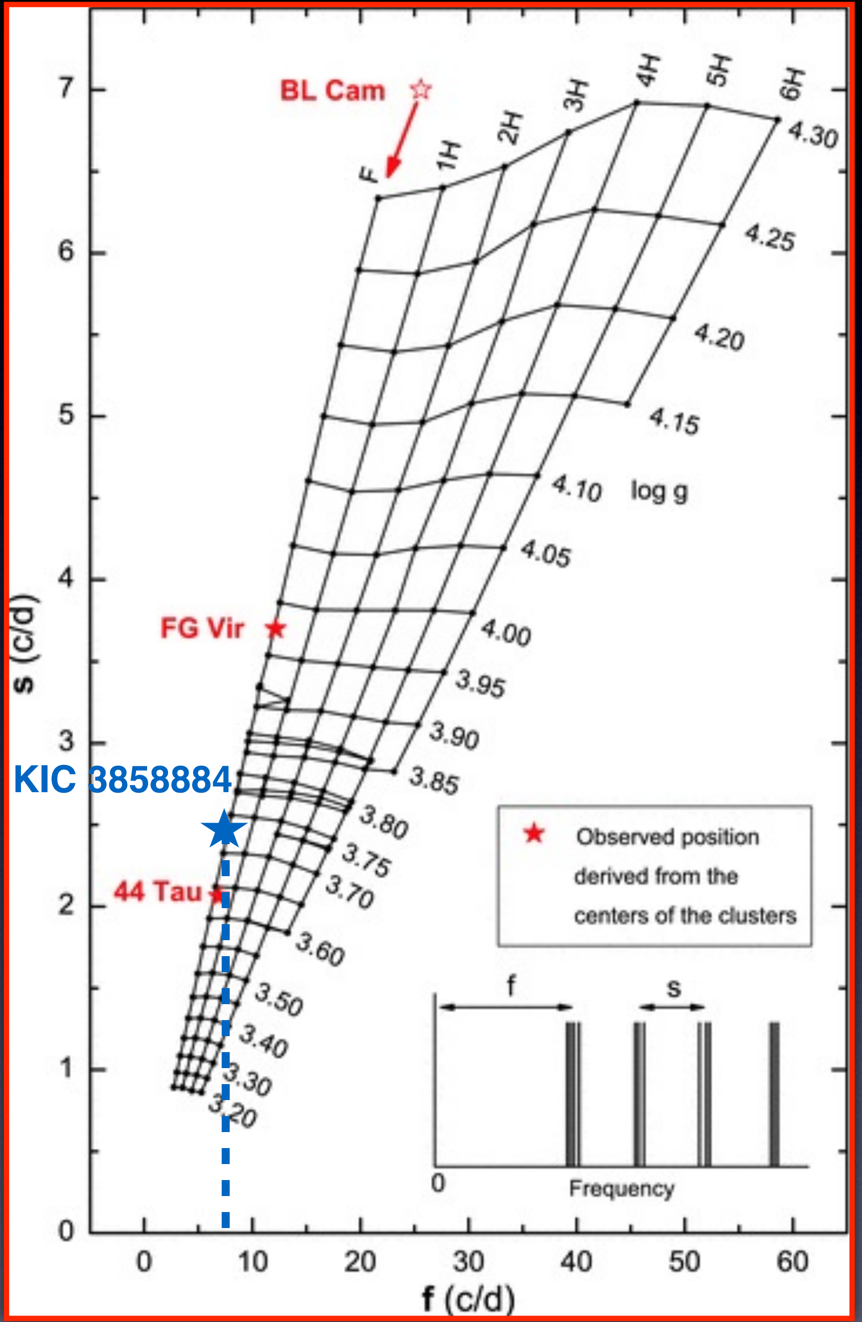

EB-SB2: <u>known log g</u> : F≅7.5 d^{-1}

- f_2 =7.47 d^{-1} : fundamental radial model
- f_1 =7.23 d^{-1} : non-radial mode

II. Low frequency variability

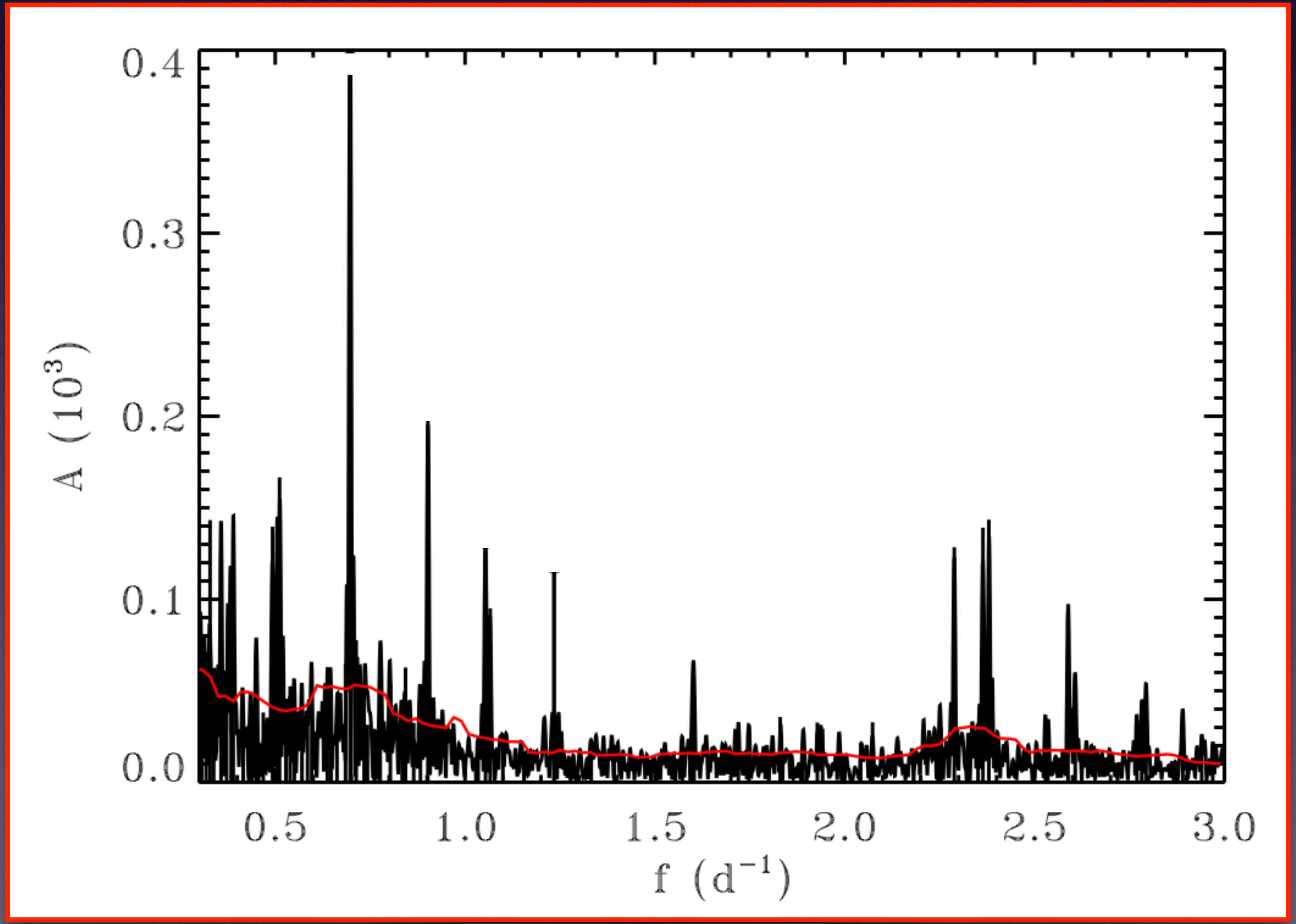

II. Low frequency variability

High order g-modes? Hybrid γ Dor - δ Sct ?

Asymptotic regime (Tassoul 1980):

$$\sigma_{n\ell} = \frac{\sqrt{\ell(\ell+1)}}{\pi(n+1/2)}\Im$$

$$\Im = \int_{r_1}^{r_2} \frac{N}{r} dr$$

Integral of the Brunt-Väisälä frequency, N, along the cavity

Moya et al. 05: (fixed l)

$$\frac{f_i}{f_j} \approx \frac{n_j+1/2}{n_i+1/2}\frac{\Im_i}{\Im_j} \approx \frac{n_j+1/2}{n_i+1/2}$$

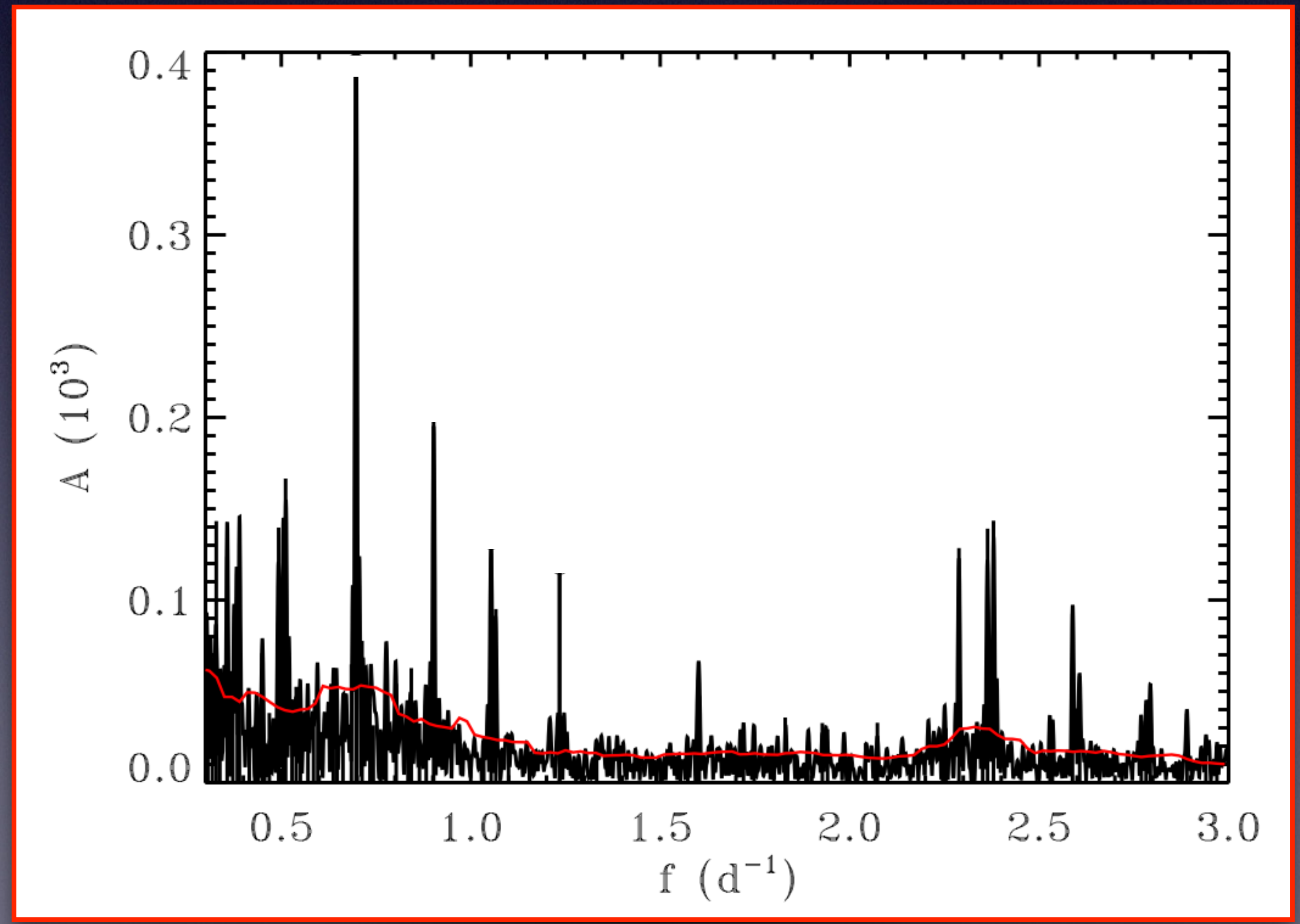

II. Low frequency variability

High order g-modes? Hybrid γ Dor - δ Sct ?

Asymptotic regime (Tassoul 1980):

$$\sigma_{n\ell} = \frac{\sqrt{\ell(\ell+1)}}{\pi(n+1/2)}\Im$$

$$\Im = \int_{r_1}^{r_2} \frac{N}{r} dr$$

Integral of the Brunt-Väisälä frequency, N, along the cavity

Moya et al. 05: (fixed l)

$$\frac{f_i}{f_j} \approx \frac{n_j+1/2}{n_i+1/2}\frac{\Im_i}{\Im_j} \approx \frac{n_j+1/2}{n_i+1/2}$$

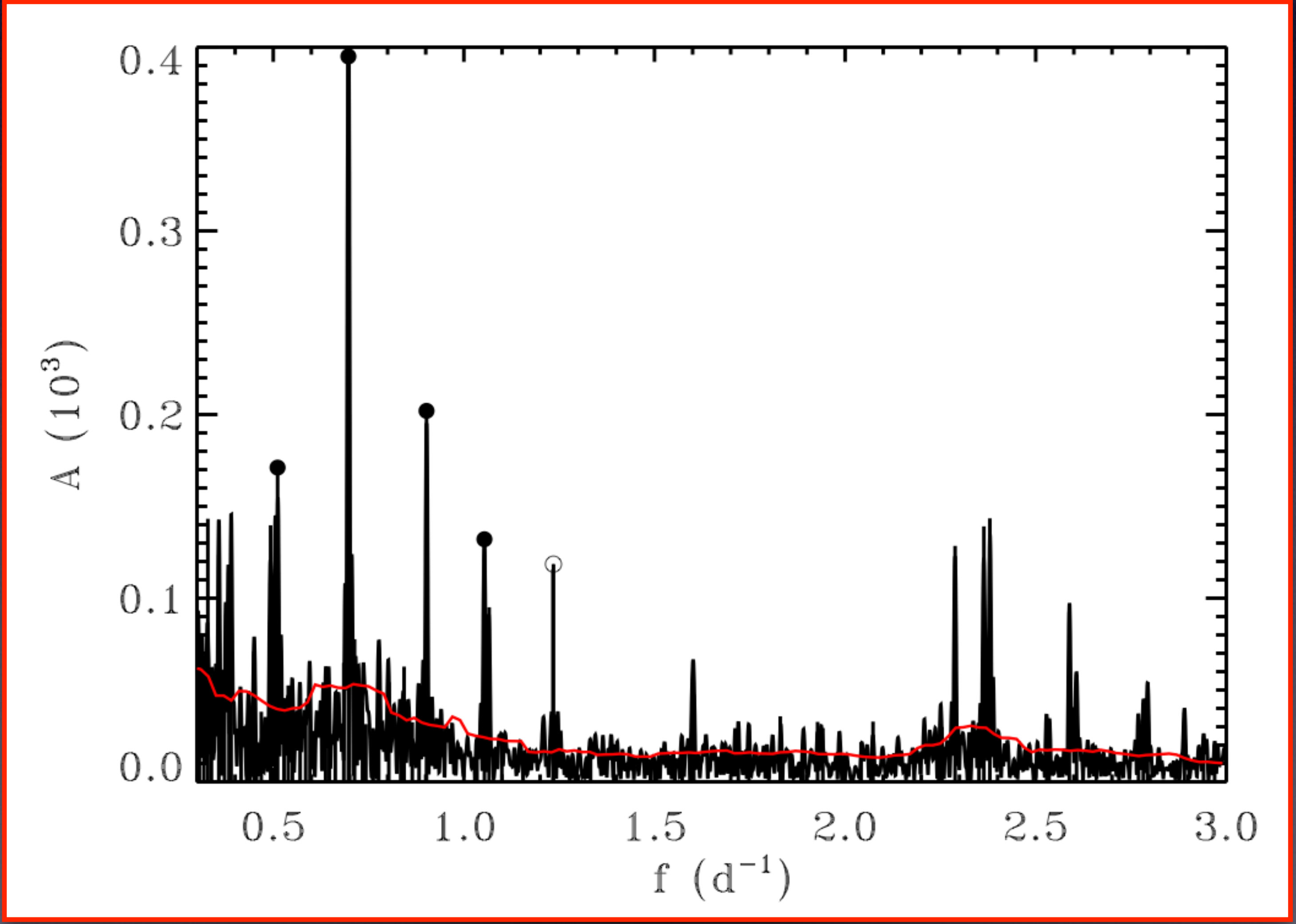

Frequency ratios (Moya et al. 05)

n_{f47} : radial order of f_{47}

ratios up to n=120

n	n	n	n	$\mathscr{I}$	$\mathscr{I}$
48	35	27	23	367.8 ± 0.4	2718 ± 3
60	44	34	29	460.8 ± 0.4	2170 ± 6
83	61	47	40	635.0 ± 1.4	1575 ± 4
85	62	48	41	648.6 ± 1.3	1542 ± 3
96	70	54	46	729.8 ± 2.1	1370 ± 4
97	71	55	47	741.6 ± 1.8	1348 ± 4
108	79	61	52	822.8 ± 1.0	1215 ± 2
109	80	62	53	834.5 ± 2.9	1198 ± 4
112	82	63	54	852.7 ± 1.7	1173 ± 2
120	88	68	58	915.7 ± 1.1	1092 ± 1

binary + evolutionary models allow to choose among the possible solutions

$\mathscr{I}$ computed assuming l=2

Frequency ratios (Moya et al. 05)

n_{f47} : radial order of f_{47} ratios up to n=120

n	n	n	n	$\mathscr{I}$	$\mathscr{I}$
48	35	27	23	367.8 ± 0.4	2718 ± 3
60	44	34	29	460.8 ± 0.4	2170 ± 6
83	61	47	40	635.0 ± 1.4	1575 ± 4
85	62	48	41	648.6 ± 1.3	1542 ± 3
96	**70**	**54**	**46**	**729.8 ± 2.1**	**1370 ± 4**
97	**71**	**55**	**47**	**741.6 ± 1.8**	**1348 ± 4**
108	79	61	52	822.8 ± 1.0	1215 ± 2
109	80	62	53	834.5 ± 2.9	1198 ± 4
112	82	63	54	852.7 ± 1.7	1173 ± 2
120	88	68	58	915.7 ± 1.1	1092 ± 1

binary + evolutionary models allow to choose among the possible solutions

$\mathscr{I}$ computed assuming l=2

Comparison with stellar models

fine grid of models around component masses with CLES (Scuflaire+08)

- EoS: OPAL05 ; opacity tables (OPAL) for two solar mixtures: GN93, AGS05
- no OV or α_{OV}=1.5, 2.0
- MLT
- different chemical compositions

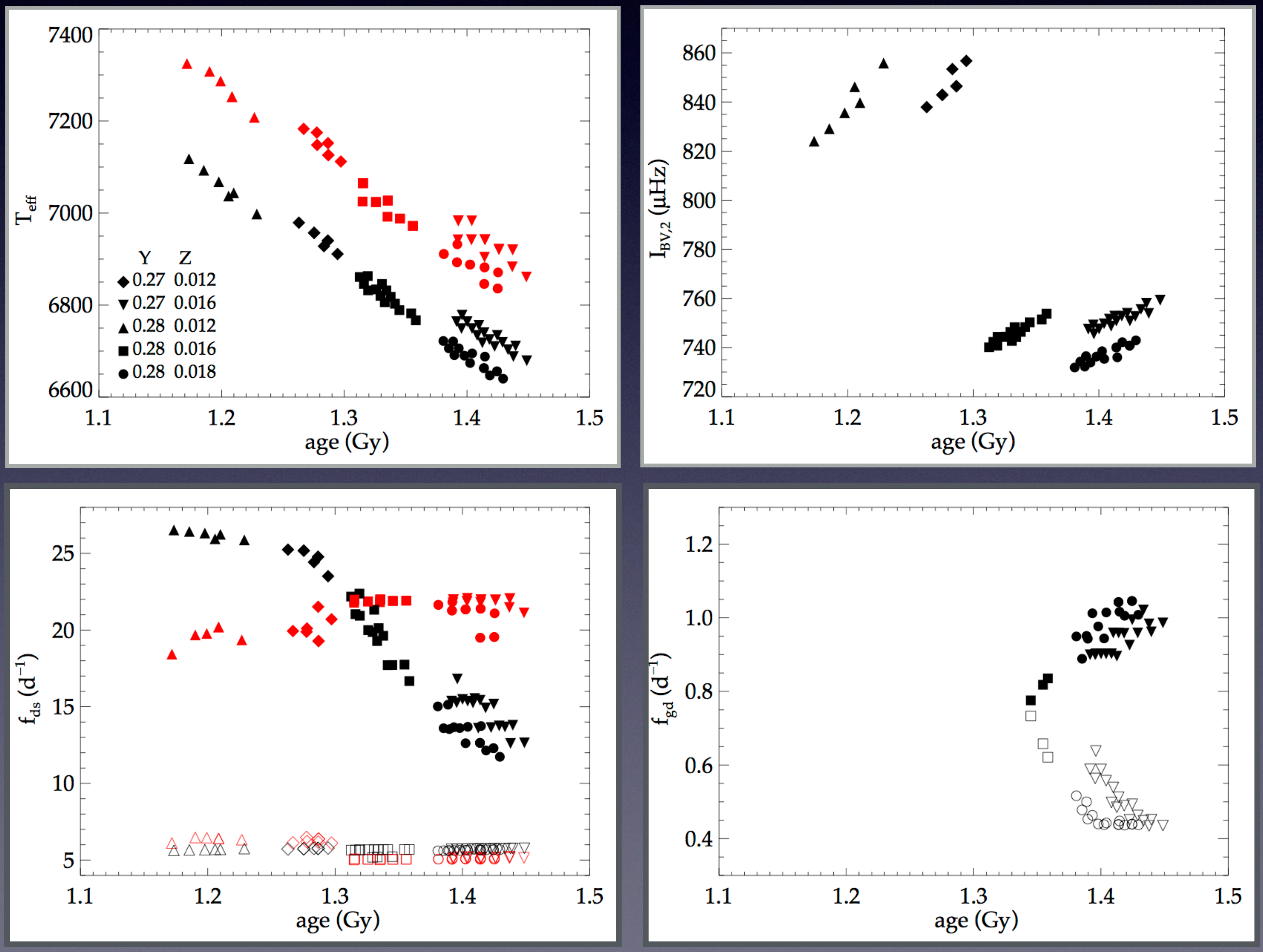

Age determination

Masses, Radii, ΔT_{eff} from the binary model

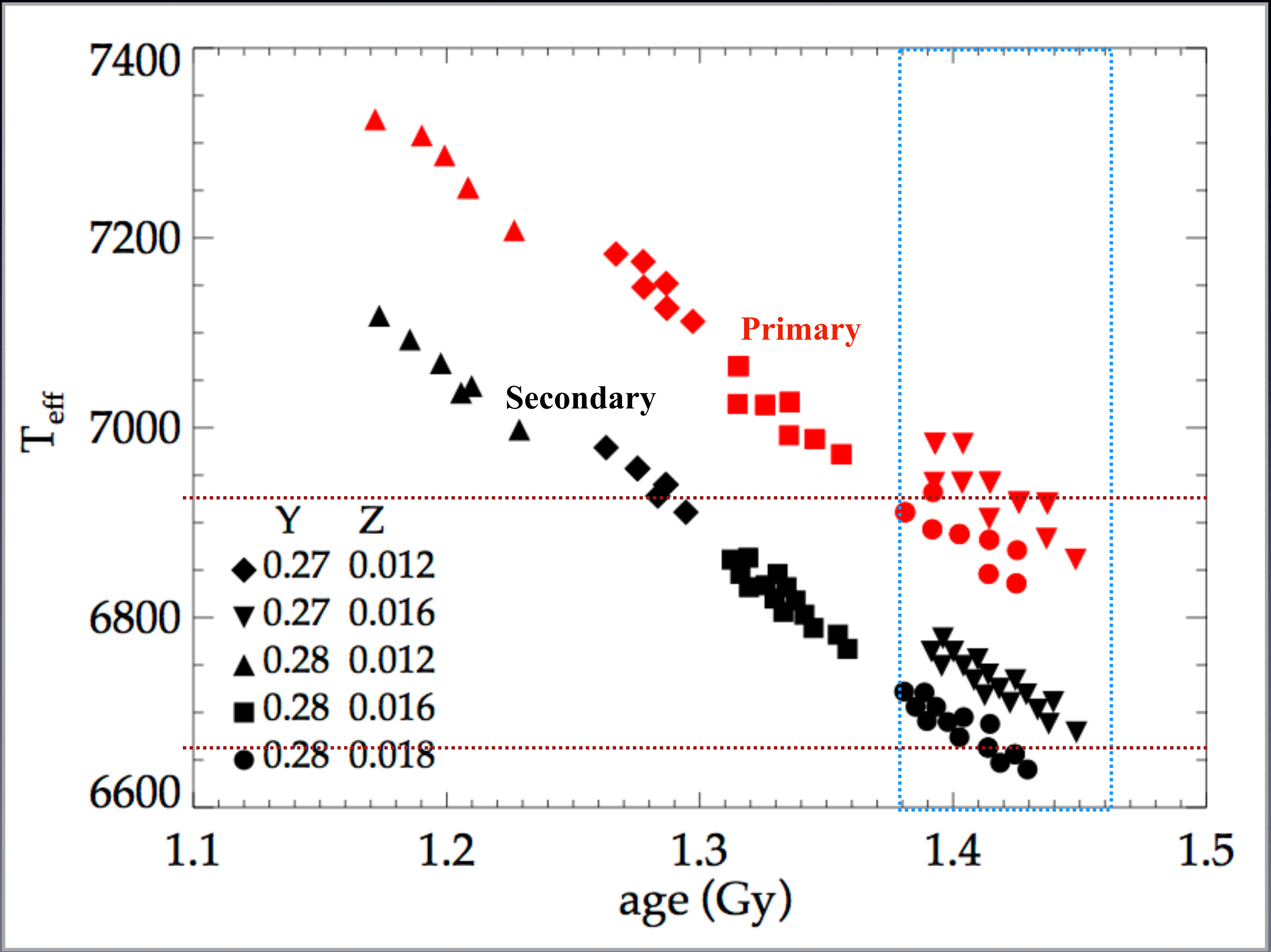

$\alpha_{OV} \neq 0$

$T_{eff,1} + \Delta T_{eff,1}$

⬇

t=1.38 –1.46 Gy

Brunt-Väisälä Integral, secondary component

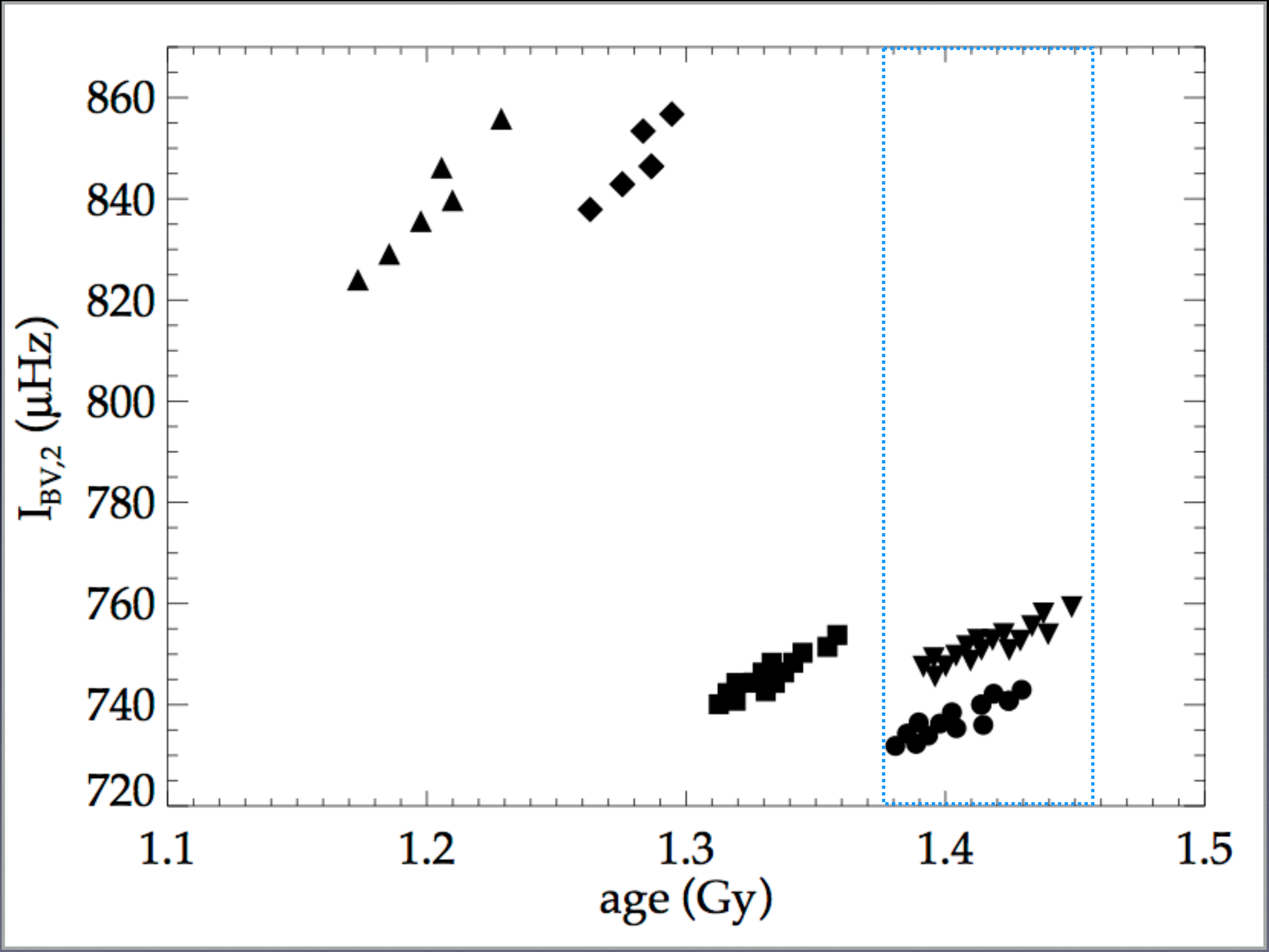

From frequency ratios:
729.8 ± 2.1
741.6 ± 1.8

Excited Frequencies: δ Sct domain

Computed with the non-adiabatic code MAD (Dupret et al. 2005)

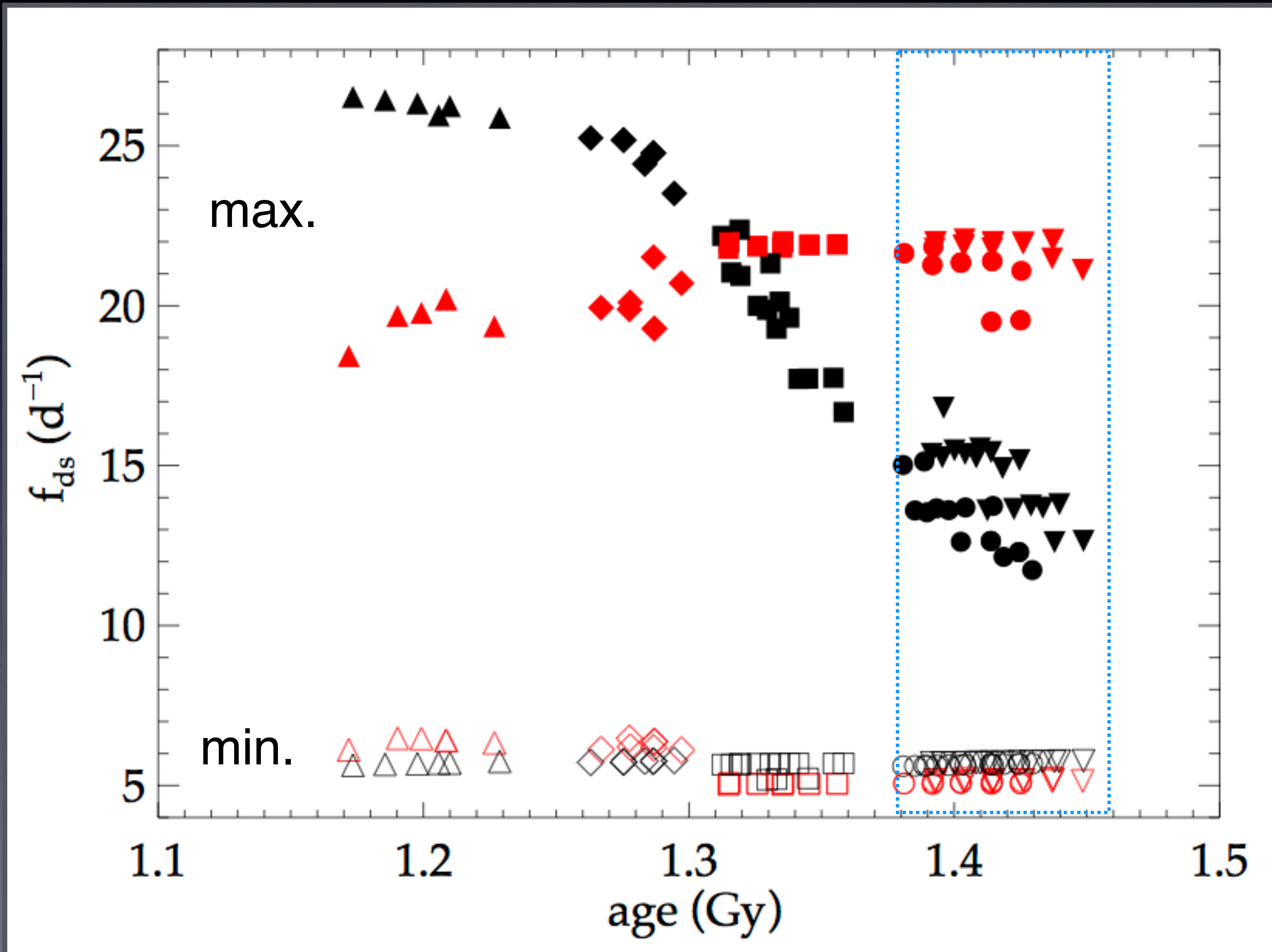

Excited Frequencies: δ Sct domain

Computed with the non-adiabatic code MAD (Dupret et al. 2005)

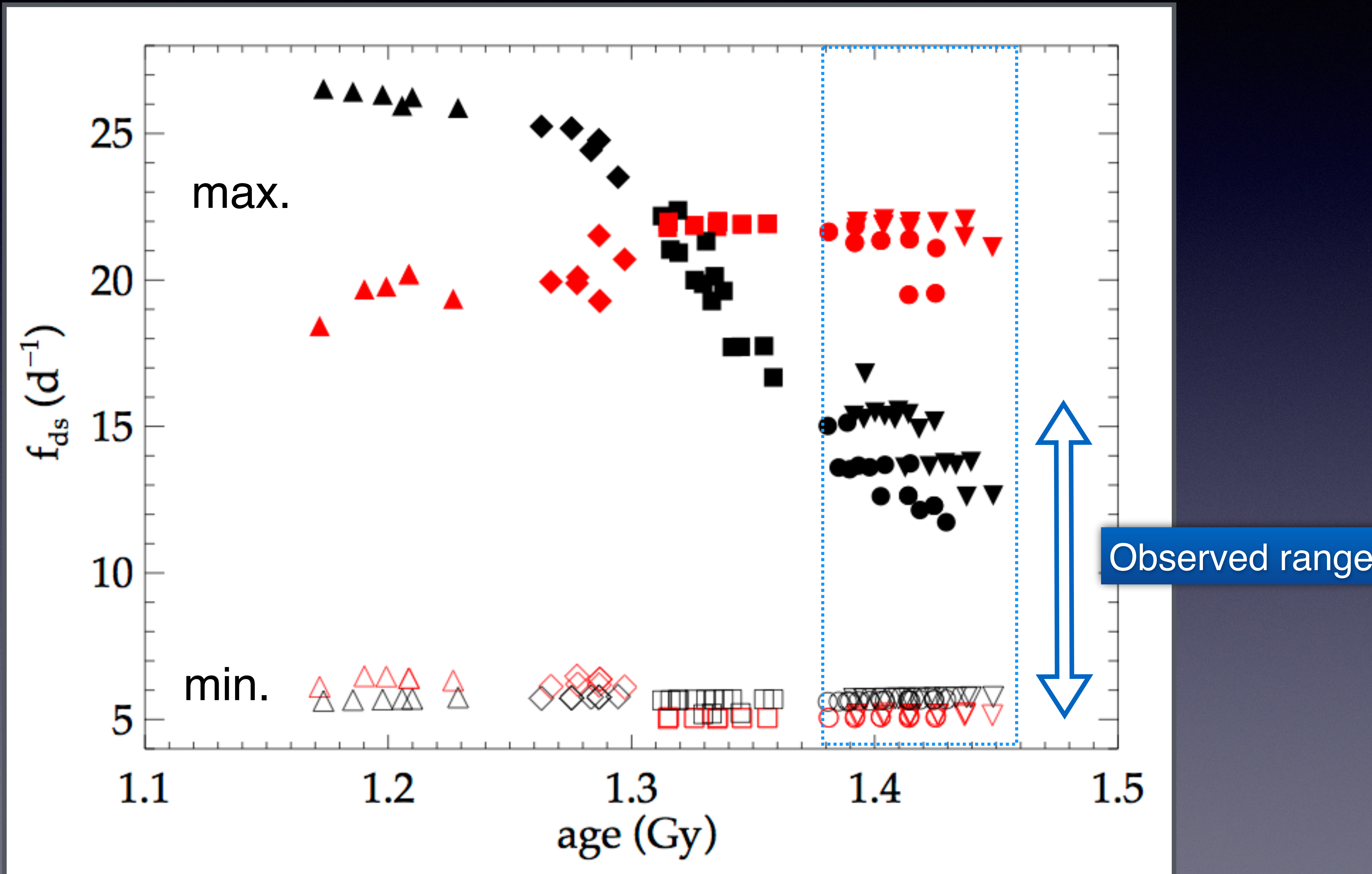

Excited Frequencies: γ Dor domain

secondary only:
excitation mechanisms is not at work in the primary

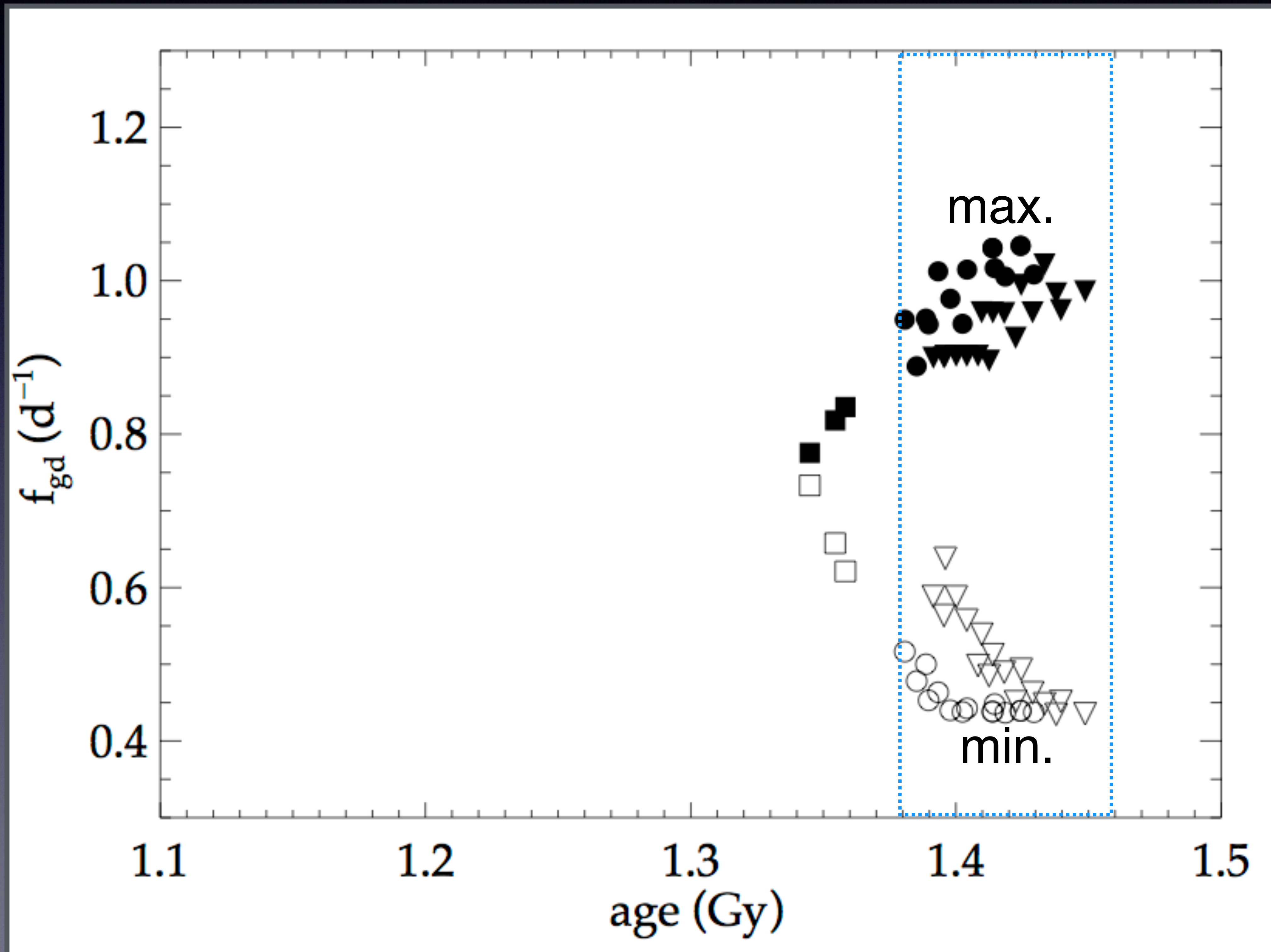

Excited Frequencies: γ Dor domain

secondary only:
excitation mechanisms is not at work in the primary

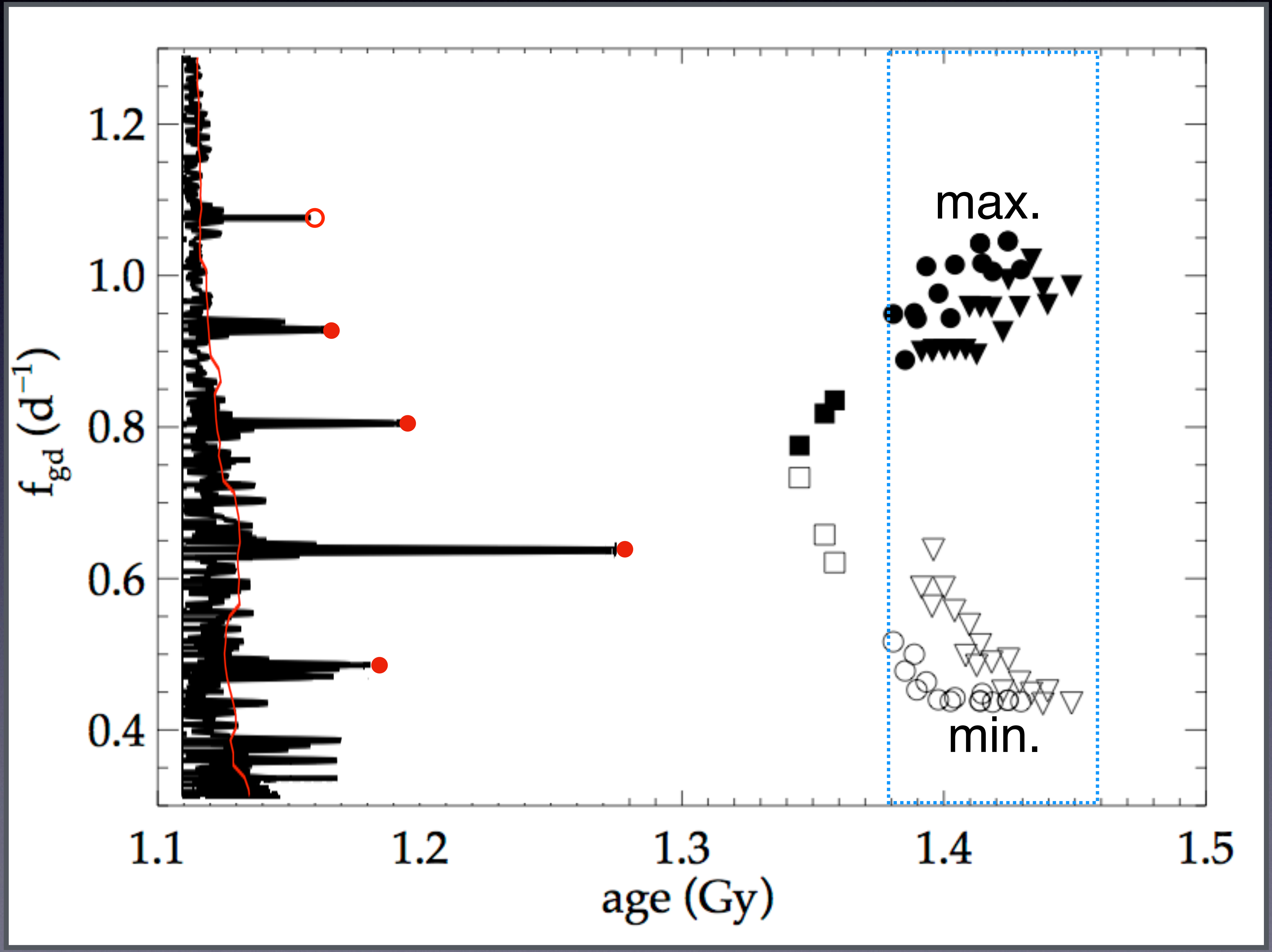

Conclusions

- EB-SB2 :
- masses, radii (log g), rotation (spin alignment)
- pulsating component
- + models: system age
  → parameter selection

- PULSATIONS:
- orbit effect (FM star)
- partial mode identification
- estimate of BV integral

Conclusions

- EB-SB2 :
- masses, radii (log g), rotation (spin alignment)
- pulsating component
- + models: system age

→ parameter selection

↔ cross validation

- PULSATIONS:
- orbit effect (FM star)
- partial mode identification
- estimate of BV integral

Conclusions

- EB-SB2 :
- masses, radii (log g), rotation (spin alignment)
- pulsating component
- + models: system age
  → parameter selection

↔ cross validation

- PULSATIONS:
- orbit effect (FM star)
- partial mode identification
- estimate of BV integral

Consistent and detailed model:
the results are worth the more complex analysis

In collaboration with:

H. Lehmann,	TLS, Tautenburg, Germany
R. Da Silva,	Univ.Tor Vergata, Rome, Italy
J. Montalbán,	free-lance, Liege, Belgium
C-U Lee,	KASSI, Daejeon, Korea
H. Ak,	Erciyes Univ., Kayseri, Turkey
R. Deshpande	Pennsylvania State University, (USA)
K. Yakut	Ege University, Izmir, Turkey
J. Desbosscher	Instituut for Sterrenkunde, K.U.L., Belgium
Z. Guo	CHARA, Atlanta (USA)
S.L. Kim	KASSI, Daejeon, Korea
J.W. Lee	KASSI, Daejeon, Korea
J. Southworth	Keele University, Keele, UK

for the full story:
A&A 563, A59 (2014)

A&A 563, A59 (2014)
DOI: 10.1051/0004-6361/201322871

Astronomy & Astrophysics

KIC 3858884: a hybrid δ Scuti pulsator in a highly eccentric eclipsing binary★,★★,★★★

C. Maceroni[1], H. Lehmann[2], R. da Silva[1], J. Montalbán[3], C.-U. Lee[4], H. Ak[5,6], R. Deshpande[6,7], K. Yakut[8], J. Debosscher[9], Z. Guo[10], S.-L. Kim[4], J. W. Lee[4], and J. Southworth[11]

1 INAF – Osservatorio astronomico di Roma, via Frascati 33, 00040 Monteporzio C., Italy
e-mail: maceroni@oa-roma.inaf.it
2 Thüringer Landessternwarte Tautenburg, Sternwarte 5, 07778 Tautenburg, Germany
3 Institut d'Astrophysique et Géophysique Université de Liège, Allée du 6 Aôut, 4000 Liège, Belgium
4 Korea Astronomy and Space Science Institute, 305-348 Daejeon, Korea
5 Erciyes University, Science Faculty, Astronomy and Space Sci. Dept., 38039 Kayseri, Turkey
6 Department of Astronomy and Astrophysics, The Pennsylvania State University, University Park, PA 16802, USA
7 Center for Exoplanets and Habitable Worlds, The Pennsylvania State University, University Park, PA 16802, USA
8 Department of Astronomy & Space Sciences, University of Ege, 35100 İzmir, Turkey
9 Instituut for Sterrenkunde, K.U. Leuven, Celestijnenlaan 200 D, 3001 Leuven, Belgium
10 Center for High Angular Resolution Astronomy and Department of Physics and Astronomy, Georgia State University, PO Box 5060, Atlanta GA 30302-5060, USA
11 Astrophysics Group, Keele University, Staffordshire ST5 5BG, UK

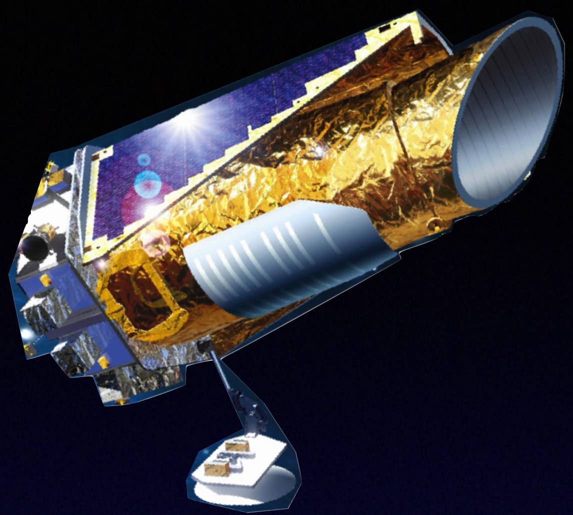

Thanks
to the CoRoT and Kepler Science teams
for making the photometry
revolution possible

....and
thank you for your attention

KIC 3858884 on the HRD